Bulletin of Engineering Geology and the Environment (2024) 83:283
https://doi.org/10.1007/s10064-024-03755-1

ORIGINAL PAPER

Assessment of undrained cyclic resistance of sand with non-plastic fines under sustained shear stress using a critical state interpretation

Giuseppe Tomasello[1] · Daniela Dominica Porcino[1]

Received: 13 November 2023 / Accepted: 21 May 2024

Abstract
There are many geotechnical applications involving dams, embankments and slopes where the presence of an initial static shear stress prior to the cyclic loadings plays an important role. The current paper presents the experimental results gathered from undrained cyclic simple shear tests carried out on non-plastic silty sand with fines content in the range 0-30% with the consideration of sustained static shear stress ratio (α). Two distinct parameters, namely the conventional state parameter Ψ, and the equivalent state parameter Ψ^*, are introduced in the context of critical state soil mechanics (*CSSM*) framework to predict failure mode and undrained cyclic resistance (*CRR*) of investigated soils. It is proved that the failure patterns for silty sands are related to (a) the initial states of soils (Ψ or Ψ^*) and (b) the combination of initial shear stress with respect to cyclic loading amplitude. At each α, the *CRR*-Ψ (or Ψ^*) correlation can be well represented by an exponential trend which is practically unique for both clean sands and silty sands up to a threshold fines content ($f_{thre}\cong$24.5%). Varying α from low to high levels simply brings about a clockwise rotation of the *CRR*-Ψ (or Ψ^*) curves around a point. This *CRR*-Ψ (or Ψ^*) platform thus provides an effective methodology for investigating the impact of initial shear stress on the cyclic strength of both clean sands and silty sands. The methodology for estimating Ψ (or Ψ^*) state parameters from in-situ cone penetration tests in silty sands is also discussed.

Keywords Silty sand · Initial static shear stress · Failure mode · Undrained cyclic resistance · State parameter · Equivalent granular state parameter

Introduction

Background and literature review

Sand-silt mixtures are very common in natural depositional environment or in earth-fill and tailings from man-made activity. The characterisation of these materials turns out to be problematic in engineering geology practice due to some peculiar features distinguishing the behaviour of these intermediate materials from that of the so called "text-book materials" (i.e. clean sands and pure clays) (Carraro and Salgado 2004). Such peculiarities include: high compressibility, intermediate values of hydraulic conductivity, different response depending on the amount and nature of fines (plastic/non plastic) and microstructure (Huang 2016). In addition, silty sands are very variable and heterogeneous in nature.

Evaluation of site response to earthquake loading and liquefaction susceptibility of low-plastic or non-plastic silty sands is fundamental but still controversial meriting further research. The main factors influencing the undrained cyclic behaviour of silty sands are fines content, packing density, stress level, grading features, and initial static shear stress. Several studies focused on the effects of fines content (f_c) on the cyclic behaviour and resistance of silty sands (Carraro et al. 2003; Chien et al. 2002; Dash and Sitharam 2009; Gobbi et al. 2022; Kuerbis et al. 1988; Porcino et al. 2021; Rahman and Sitharam 2020; Thevanayagam et al. 2002; Yang et al. 2015) but the results of these studies do not agree with each other mainly due to the fact that different parameters are used to define the initial state density, such as global void

✉ Daniela Dominica Porcino
daniela.porcino@unirc.it

Giuseppe Tomasello
giuseppe.tomasello@unirc.it

[1] Department DICEAM, Mediterranea University of Reggio Calabria, Via Zehender (Feo Vito), Reggio Calabria 89122, Italy

Published online: 21 June 2024

ratio e (Dash and Sitharam 2009; Porcino et al. 2018a, 2021; Gobbi et al. 2022; Rahman and Sitharam 2020), relative density D_R (Carraro et al. 2003; Chien et al. 2002; Gobbi et al. 2022), skeleton void ratio e_s (Carraro et al. 2003; Dash and Sitharam 2009; Kuerbis et al. 1988), and finally equivalent granular void ratio e^* (Gobbi et al. 2022; Porcino et al. 2021; Rahman and Sitharam 2020; Thevanayagam et al. 2002).

Among them, the conventional global void ratio (e), which is defined as the volume of voids divided by the volume of solids, has long been used in soil mechanics as a proper density index to describe and interpret the undrained behaviour of clean sands (Alarcon-Guzman et al. 1988; Castro and Poulos 1977; Ishihara 1993). When e is used as a control variable for sand-silt mixtures, there appears to be an agreement that the undrained cyclic resistance (*CRR*) of silty sands firstly decreased with increasing f_c up to a certain threshold value beyond which *CRR* increased thereafter for higher f_c (Polito 1999; Porcino et al. 2021; Thevanayagam et al. 2002; among others). Nevertheless, the applicability of the conventional void ratio e to silty sands has been called into question by numerous authors (Thevanayagam et al. 2002; Rahman and Lo 2008; Yang et al. 2015), based on the consideration that the study of undrained behaviour of binary granular mixtures, i.e. constituted by fine and coarse particles such as silty sands and sandy silts, requires a great understanding of microstructure which can be constituted in many different ways with different types of intergrain contacts (Thevanayagam et al. 2002). Depending on different proportions of coarse and fine grains, sand-fines mixtures can be divided into two different structures: case (*i*) fines in sand (i.e. "sand dominated") and case (*ii*) sand in fines (i.e. "fines dominated"). Therefore, there exists a f_c threshold (f_{thre}) which defines the transition from the first type of behaviour to the second one (Porcino et al. 2019; Yang et al. 2006; Zuo and Baudet 2015).

For the case (*i*), when the volume of fines content is small enough compared to that of the sand grains, the fines are regarded just to fill the void space between the sand particles and thus are practically inactive, with little contribution to supporting the coarse grain skeleton. Based on this hypothesis, the concept of an intergranular void ratio or skeleton void ratio e_s was introduced (Chu and Leong 2002; Georgiannou et al. 1990; Kuerbis et al. 1988; Pitman et al. 1994; Thevanayagam 1998). It is defined as:

$$e_s = \frac{e + f_c/100}{1 - f_c/100} \tag{1}$$

where f_c is expressed in percent.

Considering that when $f_c < f_{thre}$ some part of the fines actively takes part in the force transmission within the silty sand, especially at higher f_c, the concept of a skeleton void ratio was further adjusted and improved by introducing the equivalent granular void ratio e^* (Thevanayagam 2000) which was adopted by numerous research carried out in literature on non-plastic silty sands (Baki et al. 2014; Goundarzy et al. 2016; Porcino et al. 2021; Rahman and Sitharam 2020; Rahman 2021; Thevanayagam et al. 2002; Zuo et al. 2023). The use of the equivalent granular void ratio e^* offers a better understanding of the participation of fines in transferring and sustaining stress during undrained loading: fines can be described as particles that have partial contacts with coarse grains by forming a bridge between two coarse grains. This contribution is well captured by the fines influencing parameter "b" which appears in the equation of e^*. The definition of e^* and the determination of b value will be reported afterwards in the following section.

It should be noted that once the threshold value of f_c is reached, the fine grains are expected to play a primary role (case *ii*): the microstructure consists of fine grains skeleton with coarse grains dispersed in the fine grain matrix. An equivalent interfine void ratio e^*_f has been introduced to describe the case (*ii*) (Thevanayagam et al. 2002).

Besides fines content, the influence of grading features of fines and coarse particles can also affect the cyclic resistance of silty sands. For example, in the case of sand-dominated silty sands ($f_c < f_{thre}$), Wei et al. (2020) reported a comprehensive study based on a specifically designed experimental programme along with literature data analysis of different mixtures. It was found that a more reduction in *CRR* at the same f_c is expected with increasing particle diameter ratio χ (i.e. the ratio D_{10}/d_{50} between the diameter of sand grains at which 10% of sample is finer and the mean particle diameter of fines).

Finally, the *CRR* of silty sands is also dependent on the initial effective confining stress; in particular, it was found that the undrained cyclic resistance of silty sands decreases with increasing effective confining stress (Porcino et al. 2021; Stamatopoulos 2010; Wei and Yang 2019a) and this detrimental effect appears more pronounced for silty sands with higher fines content (Porcino et al. 2021; Stamatopoulos 2010).

However, there are many geotechnical applications, such as beneath earth dams, embankments, slopes and near-building structures, where soil elements are subjected to an initial static shear stress (τ_{stat}) on the horizontal plane, which can modify the *CRR* and the failure modes of silty sands. Case histories of liquefaction-induced failure in clean sands and silty sands in the presence of an initial static shear stress during several earthquakes were reported by Chiaro and Koseki (2013), Kokusho (2020), Porcino and Diano (2016), and Wei et al. (2018) but only a limited number of studies concern laboratory investigation of undrained cyclic

behaviour of silty sands with different f_c considering an initial static shear effect (Kokusho 2020; Pan et al. 2020, 2021; Porcino and Diano 2016; Porcino et al. 2018b; Tomasello and Porcino 2023; Wei and Yang 2019b; Wei et al. 2023; Zhou et al. 2023).

In practice, the initial static shear stress effect is usually described by introducing the parameter α, which is defined by the following equation:

$$\alpha = \tau_{stat}/\sigma'_{v0} \tag{2}$$

where σ'_{v0} and τ_{stat} are the in-situ initial vertical effective stress and static shear stress acting on the horizontal plane, respectively.

Under cyclic loading conditions, the cyclic shear stress τ_{cyc} is superimposed with τ_{stat} and applied on the soil element so that shear stress-reversal condition ($\tau_{cyc} > \tau_{stat}$) or no shear stress-reversal condition ($\tau_{cyc} \leq \tau_{stat}$) can occur causing different failure mechanisms. In particular, three typical cyclic failure mechanisms, namely flow-type failure, cyclic mobility and plastic strain accumulation, were identified based on experimental studies carried out on saturated silty sands. It was found that void ratio, effective confining stress, initial static shear stress, loading amplitude, and soil fabric are the dominant factors controlling the cyclic failure modes (Wei et al. 2023).

Similarly to clean sands, a correction factor K_α was introduced for silty sands to characterise the effect of α on cyclic resistance, based on undrained cyclic triaxial tests (Wei and Yang 2019b; Wei et al. 2023) and undrained cyclic simple shear tests (Tomasello and Porcino 2023). Based on undrained cyclic simple shear tests performed on undisturbed low-plasticity silty sand (f_c = 40%, 70%) recovered from a site where liquefaction phenomena occurred after the 2012 Emilia Romagna earthquake (Italy), Porcino and Diano (2016) discovered that static shear stress (α = 0.10) negatively affects the liquefaction potential and consequently results in a decrease in cyclic resistance. However, other researchers found that the cyclic liquefaction resistance of reconstituted silty sands either decreases or increases with increasing α, depending on the initial state (i.e. the combination of initial global void ratio and mean effective stress) of silty sand through undrained cyclic triaxial tests (Wei and Yang 2019b; Wei et al. 2023) and undrained cyclic simple shear tests (Tomasello and Porcino 2023). Zhou et al. (2023) performed a series of cyclic undrained triaxial tests on silty sands with f_c in the range 0-20% on specimens reconstituted at the same relative density ($D_R \approx 40\%$) and subjected to an effective confining stress of 100 kPa. The results suggested that the cyclic liquefaction resistance tends to monotonically increase with α, irrespective of f_c. The contradictory findings from different researchers necessitate a more comprehensive and consistent investigation into the role of initial static shear in the liquefaction behaviour of silty sand.

Since it is widely accepted that the cyclic behaviour and liquefaction resistance of clean sands and silty sands depend on the initial state, it is convenient to adopt a unified framework capable of taking into account the combined influence of void ratio and effective confining pressure in a satisfactory way. In this context, critical state soil mechanics (*CSSM*) approach has been applied to clean sands (Jefferies and Been 2016; Viana da Fonseca et al. 2022; Yan et al. 2023) and more recently to silty sands as well (Huang and Chuang 2011; Hsiao and Phan 2016; Porcino et al. 2021; Rahman and Sitharam 2020; Stamatopoulos 2010; Zuo et al. 2023) for characterising undrained monotonic and cyclic strength i.e. cyclic liquefaction resistance, static liquefaction/instability (Porcino et al. 2020; Rahman and Sitharam 2020; Stamatopoulos 2010; Zuo et al. 2023) and failure patterns (Porcino et al. 2021; Wei et al. 2023; Yang and Sze 2011a).

Different researchers proposed a variety of state indices to capture such state-dependent behaviour, but most of them considered the traditional state parameter Ψ (Been and Jefferies 1985) and the equivalent granular state parameter Ψ^* (Rahman 2012), defined hereunder, for characterising the undrained cyclic response of sands with non-plastic fines. Notably, the results of these studies from undrained cyclic triaxial tests illustrated that *1*) a unified *CRR*-Ψ (or Ψ^*) correlation (exponential or linear) can be established irrespective of packing density, confining pressure, fines content (Huang and Chuang 2011; Hsiao and Phan 2016; Rahman and Sitharam 2020; Stamatopoulos 2010; Zuo et al. 2023), and base sand with similar mineralogy (Wei and Yang 2019a). Such correlations, however, were found to depend on sample reconstitution method (i.e. soil fabric) (Huang and Chuang 2011); *2*) the use of Ψ^* may reduce the number of required tests in identifying critical state lines for sand with each f_c (Mohammadi and Qadimi 2015; Rahman and Sitharam 2020; Xu et al. 2021) and the prediction based on *CRR*-Ψ^* platform matches with the field observation (Rahman and Sitharam 2020).

Such analyses in terms of the state parameter have also been extended to characterise the undrained cyclic strength of clean sands and sands with fines in the presence of an initial static shear stress but these studies are rather limited (Wei and Yang 2019b; Wei et al. 2023; Yang and Sze 2011a, b). In the framework of critical state soil mechanics Wei et al. (2023), among others, successfully characterised the combined effects of initial static shear stress and soil fabric on the liquefaction characteristics of silty sands with different initial states. The results demonstrated that an important feature of *CRR*-Ψ relationships for clean sands and silty

sands is that they are subjected to a "clockwise rotation" when α increases.

The concept of threshold α (α_{th}) proposed by Yang and Sze (2011a) to characterise the impact of α on cyclic resistance of clean sands was proved to apply to silty sands as well (Wei and Yang 2019b). When $\alpha < \alpha_{th}$, *CRR* increases with increasing α, otherwise it decreases with increasing α. It was found that α_{th} depends on initial state and can also be characterised for various fines contents by using the initial state parameter Ψ, thus leading to a linear relationship that α_{th} decreases with increasing initial state parameter, regardless of fines contents of the mixtures.

Definitions of the framework parameters

The critical state was first mentioned by Casagrande (1936), and then defined by Roscoe et al. (1958) as a state in where soil is continuously deformed at constant stress and constant void ratio. This state is the ultimate state that will be reached when a soil is sheared. In the present work it is assumed that the critical state and the steady-state of deformation are equivalent in accordance with the literature (Been et al. 1991).

The loci of critical states form a curve in the void ratio (e)-mean effective stress (p')-deviatoric stress (q) space. The projection of critical state line in the stress plane (q, p') is a straight line passing through the origin with slope M, expressed through the equation:

$$q = M \bullet p' \tag{3}$$

where:

- q = deviatoric stress = σ_v - σ_h, with σ_v and σ_h being the total vertical and horizontal stresses, respectively.
- p'=mean effective stress=$(\sigma'_v+2\cdot\sigma'_h)/3$, with σ'_v and σ'_h being the effective vertical and horizontal stresses, respectively.
- M = critical state stress ratio.

In case of triaxial compression tests, the critical state friction angle (φ'_{cs}) can be obtained from the inclination M_c of the critical state line in the (q, p') plane using the following equation:

$$sin\phi'_{cs} = \frac{3 \bullet M_c}{6 + M_c} \tag{4}$$

The critical state friction angle depends on the uniformity of particle sizes, their shape, and mineralogy, and is developed at large shear strains irrespective of initial conditions.

Several studies on the influence of fines content on the critical state lines (*CSLs*) of silty sands in the e-logp' plane have been published in the literature (Bouckovalas et al. 2003; Carrera et al. 2011; Porcino et al. 2022; Rahman and Lo 2008; Rahman and Sitharam 2020; Thevanayagam et al. 2002; Zhu et al. 2022; Zuo et al. 2023). Interpretations of the shape and position of *CSLs* can be divided into two groups: *i*) the first one reports that *CSLs* are linear and their slopes change with changing fines content (Been and Jefferies 1985; Bouckovalas et al. 2003), *ii*) the second one shows that *CSLs* are curved and more or less parallel for different fines content (Porcino et al. 2022; Rahman and Lo 2008; Rahman and Sitharam 2020; Thevanayagam et al. 2002; Zhu et al. 2022; Zuo et al. 2023).

A curved *CSL* in the e-logp' plane was used in the present study when introducing Ψ, according to the following equation:

$$e_{CS} = e_\Gamma - \lambda_c \bullet (p'/P_a)^\xi \tag{5}$$

where:

- e_{CS} is the critical void ratio,
- e_Γ, λ_c, ξ are fitting parameters,
- P_a is the atmospheric pressure, i.e. 100 kPa.

The critical state parameters e_Γ, λ_c, ξ [Eq. (5)] and M_c [Eq. (3)] for all mixtures investigated in the current work were determined from previous research (Porcino et al. 2020) by performing undrained monotonic triaxial compression tests on the same materials tested in the present study.

Various normalised parameters have been proposed to characterise the distance between the initial state and the critical state line. Been and Jefferies (1985) have quantified the distance of the current state from the critical state line by means of a state parameter, Ψ (Fig. 1) defined as:

$$\Psi = e_0 - e_{CS} \tag{6}$$

where e_0 is the void ratio at theinitial state and e_{CS} is the critical void ratio corresponding to the current mean effective stress p'_0.

Since the current work presents and analyses tests carried out in the simple shear device, the initial mean effective stress p'_0 of each simple shear specimen was calculated considering that the initial effective horizontal stress is equal to:

$$\sigma'_{h0} = K_0 \bullet \sigma'_{v0} \tag{7}$$

$$K_0 = 1 - \sin(\phi') \tag{8}$$

where K_0 is the coefficient of lateral earth pressure at rest.

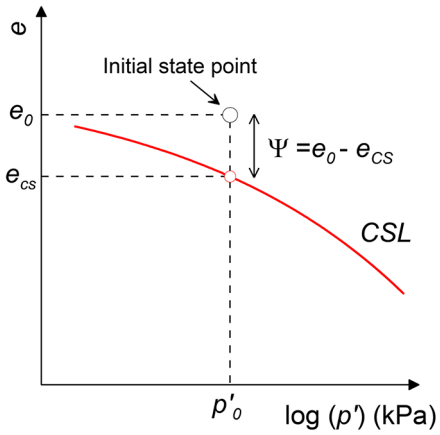

Fig. 1 Critical state line and definition of state parameter

If the critical state friction angle φ'_{cs} is introduced in Jaky's equation [Eq. (8)], K_0 is unique for a given Ticino-silt mixture, regardless of density state and results in the range 0.38–0.43, the lower value refers to clean Ticino sand (φ'_{cs}=35°) and the higher value refers to *TS*+30% fines content (φ'_{cs} =38°). It should be noted that when different values of φ' (φ'_p against φ'_{cs}) are employed in Eq. (8), it was verified that the variation in K_0 values is poorly significant for the purpose of calculating state parameter.

It is noteworthy that the *CSL* for a specific silty sand is not dependent on the applied stress path and therefore the *CSL* obtained from undrained monotonic triaxial tests can be applied in the present study to the analysis of simple shear test data as well.

According to the definition of the state parameter Ψ, soils that have an initial state above the *CSL* with $\Psi > 0$ show contractive behaviour, whereas soils with the initial state below the *CSL* and $\Psi < 0$ show a dilative response.

As discussed earlier, the equivalent granular void ratio e^* (Thevanayagam 2000) represents a superior parameter in lieu of e to characterise the mechanical behaviour of non plastic silty sands with $f_c < f_{thre}$. It is defined as:

$$e^* = \frac{e + (1-b) \bullet f_c/100}{1 - (1-b) \bullet f_c/100} \tag{9}$$

where b indicates the portions of fine particles that participate in the active intergrain contacts ($0 \le b \le 1$): $b=0$, would mean that none of the fine grains actively participates in supporting the coarse-grain skeleton and thus the Eq. (9) for e^* reduces to Eq. (1) for e_s; $b=1$ would mean that all of the fine grains actively participate in supporting the coarse grain skeleton.

The fines influencing factor b accounts for all the combined effects of different parameters on the undrained response of sand due to the addition of fines (Rees 2010). The prediction of b factor is a critical issue for the application of the e^*-based approach to silty sands with $f_c \le f_{thre}$. Previous studies stated that b is affected by several factors, such as grading features of sand-silt mixtures (Goundarzy et al. 2016; Mohammadi and Qadimi 2015; Ni et al. 2004), fines content (in general normalised to the threshold fines content, f_c/f_{thre}) (Goundarzy et al. 2016; Lashkari 2014; Rahman and Lo 2008), mineralogy and angularity of particles as well (Lashkari 2014; Rees 2010). Only a few authors have examined the impact of loading type (cyclic vs. monotonic) on the variation of b (Porcino et al. 2022; Rees 2010).

Various approaches to estimate b parameter are reported in the literature. Several researchers assumed the b parameter varies with grading features and determined a single b value using back analysis for mixtures of sand with different fines contents (Ni et al. 2004; Thevanayagam and Martin 2002). Following this approach, simple relationships between the b parameter and grading features of sand-fines mixtures were proposed (Mohammadi and Qadimi 2015; Rees 2010). On the other hand, other authors (e.g., Porcino et al. 2021; Rahman and Lo 2008; among others) considered the dependence of the b parameter on fines content. In this regard, back-analysing different databaset reported in the literature, Rahman and Lo (2008) proposed a semi-empirical equation to estimate b as a function of f_c and grading features of the mixtures as well. In the present study, a unique value of b for all sand-fines mixtures was considered in the analysis of the results for ease of application of the e^*-based approach in the presence of an initial shear stress.

The concept of e^* is inherently assumed that the critical state data points for sand with fines will come to a single critical state line in e^*-logp' plane (called "equivalent granular critical state line", *EG-CSL*) for different fines content ($f_c \le f_{thre}$) (Porcino et al. 2022; Rahman and Lo 2008; Thevanayagam et al. 2002). The assessment of an *EG-CSL* in the e^*-logp' space allows the introduction of a modified state parameter, defined equivalent granular state parameter, Ψ^*, for the analysis of the undrained monotonic and cyclic behaviour of silty sands. It is defined as:

$$\Psi^* = e^* - e^*_{CS} \tag{10}$$

where e^* and e^*_{CS} are the equivalent void ratio and the critical equivalent void ratio at the same p'. The Ψ^* at the beginning of a test is called initial equivalent granular state parameter ($\Psi^*_{(0)}$).

Scope and novelty of this study

Very little effort has been devoted to experimental and theoretical research of silty sands in presence of an initial static shear stress. Additionally, all the relationships reported in the literature between undrained cyclic resistance and state parameter were derived from conventional cyclic

triaxial tests while it is recognised that simple shear apparatus, employed in the present study, is able to reproduce in a satisfactory way the stress conditions in field soil elements before and during earthquakes even with the presence of τ_{stat}.

This paper presents a systematic experimental program of undrained cyclic simple shear (*CSS*) tests conducted on sand-silt mixtures tested at various initial states (void ratio, vertical effective stress, static shear stress) with fines content less than the threshold value (i.e. the soil behaviour is primarily dominated by the coarse grain skeleton). A unified framework based on critical state soil mechanics (*CSSM*) is put forward to characterise the undrained cyclic resistance and failure patterns of sand-silt mixtures in the presence of a sustained shear stress. Besides using the traditional state parameter Ψ, test results have also been analysed by introducing a new platform based on the equivalent granular state parameter Ψ^*.

One of the most relevant findings of the study is that α-induced clockwise rotation of the *CRR*-Ψ (Ψ^*) curves shall apply to silty sands under cyclic simple shear loading conditions. The proposed approach for assessing liquefaction potential of silty sands appears promising over the conventionally adopted semi-empirical field-based simplified procedure which requires the determination of the two correction factors, K_α and K_σ. The assessment of these two factors, however, is still uncertain for design purposes especially in silty sands.

Material and test program

Two materials were adopted in the experimental investigation for the preparation of soil mixtures, namely (1) the clean Ticino sand, and (2) a non-plastic silt. Ticino sand is a uniform coarse-to-medium natural silica sand comprising sub-rounded to sub-angular grains recovered from the Ticino River; the fines is a natural non-plastic silt collected from the same site.

The grain size distribution curves of the tested soils are presented in Fig. 2, while the basic physical properties are reported in Table 1. For the mixtures tested in the present study, the particle diameter ratio χ was equal to 17 for *TS*-fines mixtures.

The testing program comprises 156 constant-volume cyclic simple shear (CSS) tests performed at (1) different values of the (global) void ratio (e_0) at the end of consolidation, ranging from 0.49 to 0.82; (2) two different values of effective vertical stress (σ'_{v0}) equal to 50 and 100 kPa; (3) different values of initial static shear stress ratio (α) ranging from 0 to 0.30; and (4) four sand-fines mixtures with fines contents f_c = 0%, 10%, 20%, 30%, by weight and the corresponding mixtures were labelled as *TS*, *TS10*, *TS20*, and *TS30*. The testing program is given in Table 2.

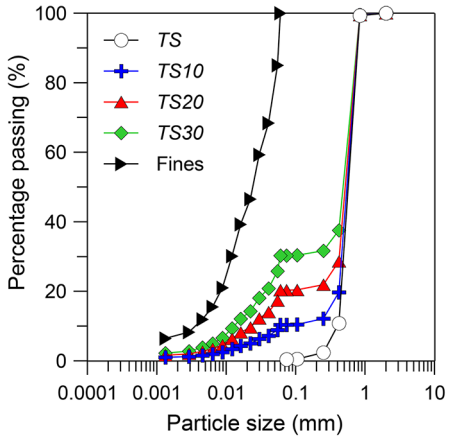

Fig. 2 Grain size distribution curves of Ticino sand-silt mixtures

Table 1 Material properties

Material	G_S	D_{50} (mm)	C_U	e_{max}	e_{min}
TS	2.68	0.564	1.48	0.93	0.58
TS10	2.67	0.547	10.16	0.81	0.47
TS20	2.68	0.518	24.69	0.79	0.37
TS30	2.69	0.483	41.55	0.80	0.37
Fines	2.72	0.024	8.54	-	-

Note: G_S=specific gravity, D_{50}=mean grain size, C_U=uniformity coefficient, e_{max}=maximum void ratio, e_{min}=minimum void ratio

The experimental tests were performed using a modified Norwegian Geotechnical Institute (*NGI*)-type direct simple shear (*DSS*) device (Porcino et al. 2006). In this *DSS* device, a steel-wire reinforced rubber membrane prevents lateral strains; consequently, a constant-volume condition is attained during loading phase by keeping the height of the sample constant. The diameter and height of specimen were equal to 80 mm and 20 mm, respectively (Fig. 3). The condition of constant sample height was performed by applying a decrease (or increase) of vertical stress ($\Delta\sigma_v$) through a closed loop control system receiving feedback from the vertical displacement transducer. It is demonstrated that $\Delta\sigma_v$ applied in a constant-volume simple shear (*SS*) test on

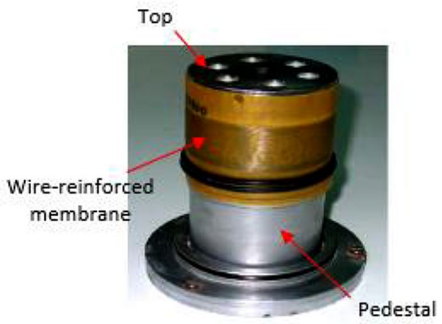

Fig. 3 Picture of soil sample after preparation and before consolidation in simple shear apparatus

Table 2 Program of constant-volume cyclic simple shear tests

f_c (%)	e_0	σ'_{v0} (kPa)	α	CSR	Number of tests
0	0.78	100	0	0.12–0.20	4
0	0.74	100	0	0.12–0.18	4
0	0.68	100	0	0.14–0.23	5
0	0.63	100	0	0.20–0.25	3
0	0.60	100	0	0.23–0.26	2
0	0.82	50	0	0.15	1
0	0.78	100	0.05	0.07–0.14	2
0	0.78	100	0.10	0.08–0.14	4
0	0.68	100	0.10	0.16–0.22	3
0	0.60	100	0.10	0.23–0.28	3
0	0.73	50	0.10	0.15–0.17	2
0	0.78	100	0.20	0.10–0.12	2
0	0.68	100	0.20	0.16–0.20	2
0	0.60	100	0.20	0.20–0.28	3
0	0.78	100	0.30	0.10–0.12	2
0	0.68	100	0.30	0.16–0.18	2
0	0.60	100	0.30	0.22–0.28	2
10	0.68	100	0	0.10–0.16	4
10	0.60	100	0	0.14–0.20	3
10	0.55	100	0	0.14–0.20	3
10	0.53	100	0	0.16–0.19	2
10	0.68	50	0	0.14–0.18	3
10	0.60	50	0	0.16–0.18	2
10	0.68	100	0.05	0.14–0.16	2
10	0.68	100	0.10	0.08–0.12	3
10	0.60	100	0.10	0.14–0.19	3
10	0.55	100	0.10	0.17–0.22	2
10	0.68	50	0.10	0.10–0.18	3
10	0.68	100	0.20	0.08–0.10	2
10	0.60	100	0.20	0.12–0.16	3
10	0.55	100	0.20	0.18–0.23	2
10	0.68	50	0.20	0.14–0.16	2
10	0.68	100	0.30	0.03–0.06	2
10	0.60	100	0.30	0.08–0.12	3
10	0.55	100	0.30	0.16–0.18	2
10	0.68	50	0.30	0.10–0.14	2
20	0.68	100	0	0.08–0.12	3
20	0.58	100	0	0.12–0.16	3
20	0.55	100	0	0.14–0.20	3
20	0.51	100	0	0.14–0.19	4
20	0.58	50	0	0.14–0.15	2
20	0.68	100	0.10	0.04–0.10	3
20	0.59	100	0.10	0.10–0.12	2
20	0.55	100	0.10	0.14–0.20	3
20	0.59	100	0.20	0.08–0.10	2
20	0.55	100	0.20	0.13–0.16	2
20	0.60	100	0.30	0.03–0.06	2
20	0.55	100	0.30	0.14–0.16	2
30	0.68	100	0	0.08–0.14	4
30	0.58	100	0	0.12–0.18	3
30	0.55	100	0	0.16–0.20	2
30	0.49	100	0	0.20–0.24	3
30	0.68	50	0	0.12–0.18	3
30	0.68	100	0.10	0.06–0.10	2
30	0.59	100	0.10	0.10–0.12	2

Table 2 (continued)

f_c (%)	e_0	σ'_{v0} (kPa)	α	CSR	Number of tests
30	0.55	100	0.10	0.16–0.19	2
30	0.68	50	0.10	0.08–0.12	2
30	0.59	100	0.20	0.08–0.10	2
30	0.55	100	0.20	0.14–0.16	2
30	0.55	100	0.30	0.12–0.14	2
30	0.60	100	0.30	0.03–0.05	2

normally consolidated clays (Dyvik et al. 1987) as well as on sands (Finn and Vaid 1977; Finn 1985; Moussa 1975) is essentially equal to the increase (or decrease) of excess pore water pressure (Δu) in a truly undrained *SS* test where the constant-volume condition is performed by a closed drainage system.

In the present study, all specimens (f_c=0-30%) were prepared to the desired void ratio by moist tamping method in two layers: the layer height was 10 mm so that it was not necessary to use the under-compaction method introduced by Ladd (1978). Dry sand and fines were first mixed at the prefixed weight ratio and afterwards an amount of de-aired water was added to the mixture to achieve 12.5% moisture content (w). Finally, the reinforced membrane was filled with the mixture in a wet condition and each layer was compacted by a system able to ensure the target final height of soil layer. The value of w was chosen because it allows to prepare specimens over a greater range of void ratios.

Different load increments were applied up to the prefixed value of vertical stress σ'_{v0} (i.e., 50 kPa or 100 kPa) during the consolidation phase. After the end of the staged consolidation, when it was necessary, the specimens were subjected under drained conditions to static shear stress (τ_{stat}) acting on the horizontal plane to reach the desired shear stress ratio value ($\alpha = \tau_{stat}/\sigma'_{v0}$). In the following analysis, the post-consolidation void ratio e_0 corresponds to the void ratio prior to and during cyclic shearing. An accuracy of about ± 0.0015 in terms of void ratio was obtained using the displacement sensors applied in the *DSS* device. The sample vertical displacements were measured using an LVDT (linear variable differential transducer, model W10TK, manufactured by H.B.M.) having a measuring range of 20 mm.

The cyclic shear stress (τ_{cyc}) corresponding to a desired cyclic stress ratio $CSR = \tau_{cyc}/\sigma'_{v0}$ was applied at a frequency of 0.10 Hz which was chosen to ensure a good control of undrained/constant volume test conditions (Porcino et al. 2006). A data acquisition system connected to a computer allowed for a continuous record of all measured data. The attainment of a single amplitude shear strain (γ_{SA}) or a peak shear strain (γ_{peak}) in the order of 3.75% was selected for detecting the initial failure condition.

Undrained cyclic resistance of silty sand with the presence of initial static shear stress

Effect of non-plastic fines content

A reference earthquake of magnitude M_w=7.5, corresponding to 15 equivalent number of uniform cycles, is generally adopted for liquefaction analyses (Idriss and Boulanger 2006; Youd et al. 2001). Figure 4 provides the relationship between undrained cyclic resistance $CRR_{N=15}$, i.e. the cyclic stress ratio (*CSR*) causing failure in 15 uniform loading cycles, and fines content (f_c) derived from the experimental data of sand-silt mixtures tested at the same initial state (e_0, σ'_{v0}) for different α levels.

Apparently, as shown in Fig. 4 for both $\alpha = 0$ and $\alpha \neq 0$, cyclic resistance values decrease with f_c up to a threshold fines content ranging between 20% and 30%; on the other hand, for higher fines content, the trend is reversed. The decrease of $CRR_{N=15}$ with f_c is much more pronounced for tests with an initial static shear stress ($\alpha \neq 0$) compared to those with absence of α.

The identification of f_{thre} was conducted considering the minimum of the fitting curves of experimental data for each α level, as sketched in Fig. 4. It was recognised the presence of a narrow-bounded zone where a unique average f_{thre} value, approximately equal to 24.5%, could be assumed for all α values (Fig. 4).

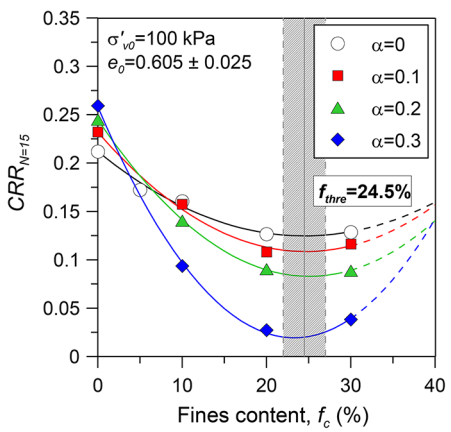

Fig. 4 Effects of fines content on cyclic resistance of silty sands for different α levels

Effect of void ratio and vertical effective stress

Relationships between the initial (global) void ratio (e_0) and the cyclic resistance ratio ($CRR_{N=15}$) for different soil mixtures tested in this study are presented in Fig. 5. All samples were consolidated at the same vertical effective stress (σ'_{v0}=100 kPa). As it can be argued from data reported in Fig. 5, the cyclic resistance ratio decreases with increasing void ratio for all mixtures and α levels. However, the impact of the change in void ratio on *CRR* is more significant for higher α values than for lower ones, regardless of fines content. A similar experimental evidence was also observed from anisotropically undrained cyclic triaxial tests performed on Toyoura sand mixed with non-plastic silt (f_c=0-20%) by Wei and Yang (2019b) among other authors. A possible explanation for the observed behaviour is that when the applied initial static shear stress increases, the materials' brittleness increases (Sivathayalan and Ha 2011; Keyhani and Haeri 2013), meaning that the behaviour of silty sand greatly softens and appears to be more contractive, particularly at low packing densities and high fines content (Fig. 5d).

Another factor influencing the cyclic liquefaction resistance of silty sands is the initial effective vertical stress (σ'_{v0}). Figure 6 shows the effect of initial vertical effective stress on *CRR* curves for two mixtures (*TS10* and *TS30*) tested at the same global void ratio and two values of α [Fig. 6(a) and 6(c), $\alpha=0$; Fig. 6(b) and 6(d), $\alpha=0.1$]. Figure 6 highlights that the cyclic resistance against liquefaction decreases as the effective vertical stress increases whatever the value of initial static shear stress is considered. A more apparent reduction of the cyclic resistance due to the effect of σ'_{v0} is observed when an initial static shear stress is applied for *TS10*; on the contrary, for the mixture characterised by a higher percentage of fines (*TS30*), a minor reduction of the cyclic resistance due to the effect of σ'_{v0} is observed when an initial static shear stress is applied. The mutual dependence of the cyclic resistance on both the initial vertical effective stress and the initial static shear stress for a given mixture was already highlighted in previous studies carried out on clean sands (Park et al. 2020; Sivathayalan and Ha 2011; Vaid et al. 2001).

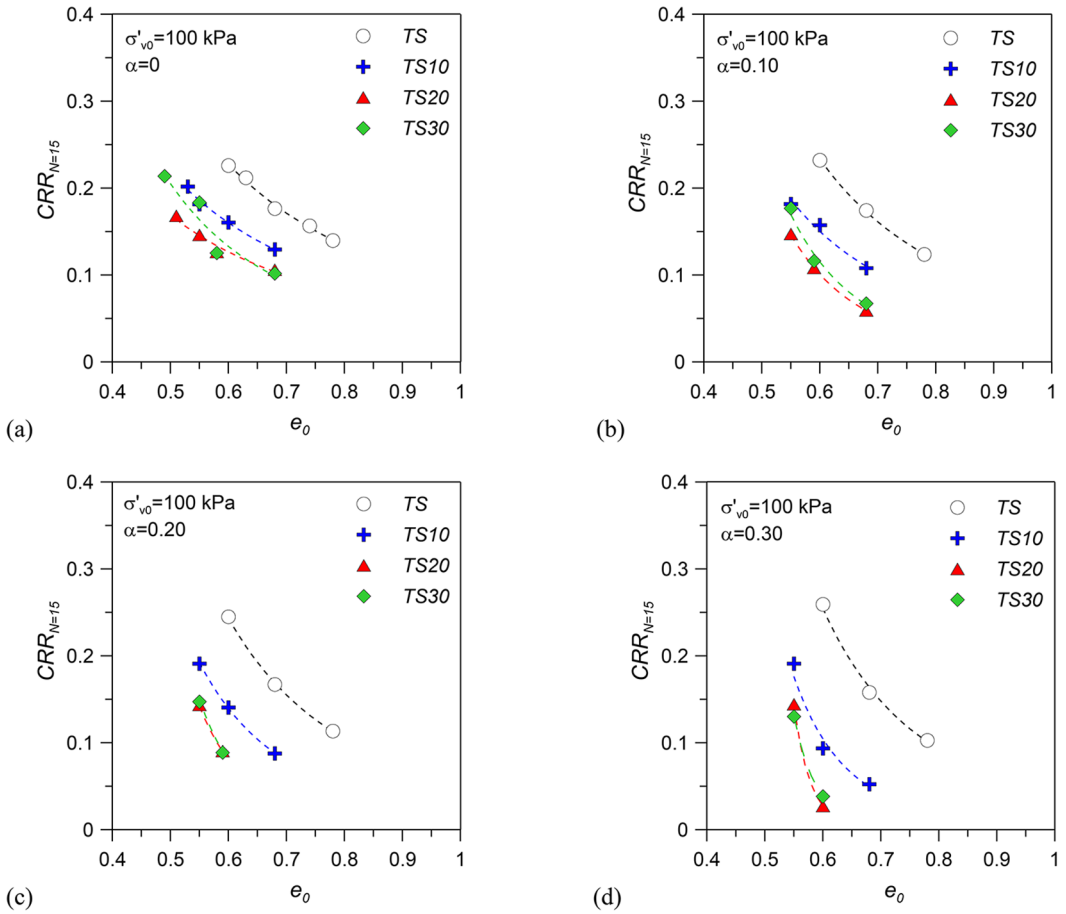

Fig. 5 Effects of post-consolidation void ratio on undrained cyclic resistance of silty sands for various f_c and α levels.

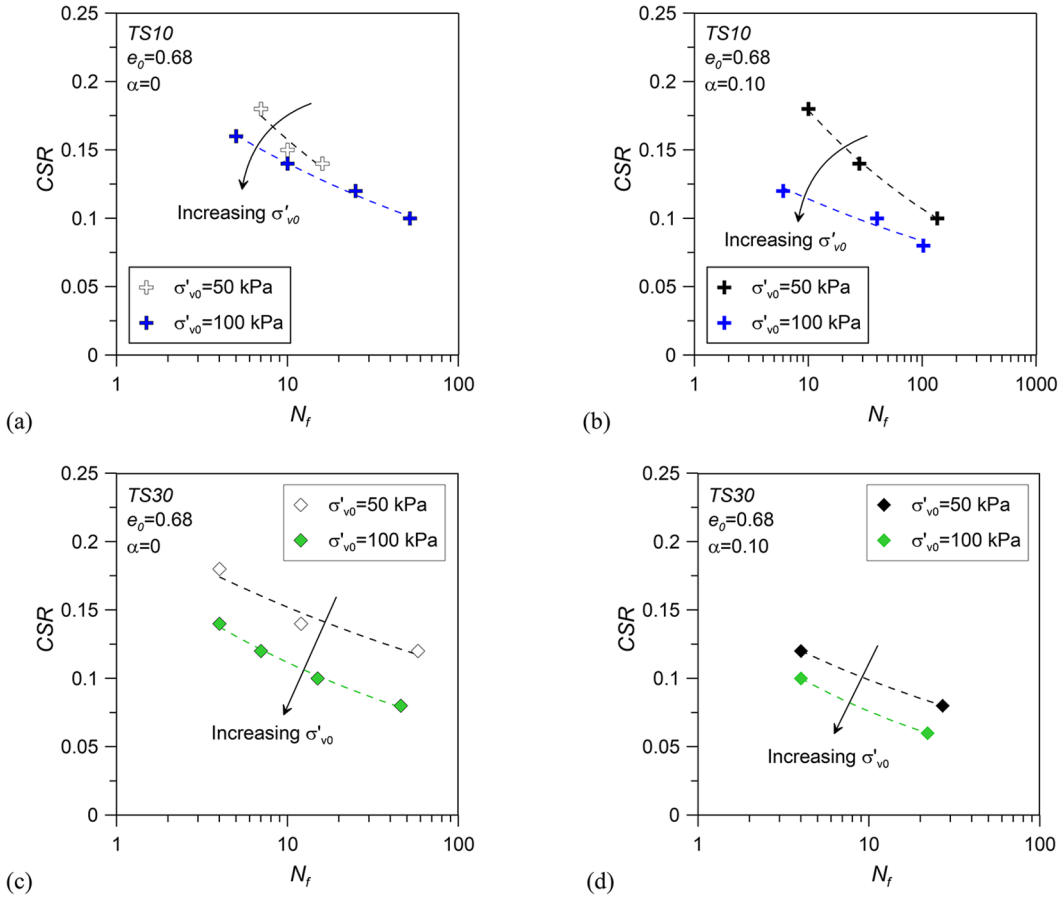

Fig. 6 Effects of initial vertical effective stress on cyclic resistance of silty sands for two different α values: (a) and (c) α=0; (b) and (d) α=0.10

CRR - Ψ correlations under an initial static shear stress

Since the undrained cyclic response of sand-silt mixtures was found to depend on the aforementioned factors, such as fines content, void ratio, effective vertical stress and initial static shear stress, a unified critical state approach based on state parameter was initially adopted. The critical state lines (*CSLs*) in the *e*-log*p′* plane (Porcino et al. 2020) are shown in Fig. 7 for all *TS*-silt mixtures. Such curves are represented by Eq. (5) with the coefficient of determination R^2 reported in Table 3.

Figure 7 indicates that *CSLs* in *e*–log*p′* plane move downwards from the clean sand to sand with 30% fines content, indicating a more contractive response of sand with a higher amount of fines. The position of the *CSLs* is controlled by e_Γ [Eq. (5)], which decreases with increasing f_c, as shown in Table 3. On the other hand, as expected from previous studies (Gobbi et al. 2022; Rahman and Lo 2014; Yang et al. 2015), the other two parameters namely λ_c and ξ were maintained constant and calculated from f_c=10% for which data are well arranged in a large p' range. It was demonstrated from previous research conducted by the authors on *TS*-fines mixtures that the value of f_{thre} based on change of critical state parameters with fines content was slightly higher than that obtained from cyclic tests (Porcino et al. 2019).

Using Eq. (6), the state parameter for all specimens of *TS*-fines mixtures tested in undrained cyclic simple shear apparatus at different void ratios and effective vertical stresses

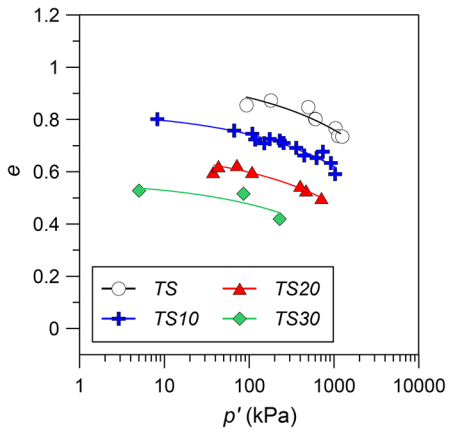

Fig. 7 Effects of fines content on critical state lines for TS-fines mixtures in *e-p′* plane

Table 3 Fitting parameters of the critical state lines for Ticino sand-fines mixtures

Material	e_Γ	λ_c	ξ	R^2
TS	0.976	0.093	0.365	0.87
TS10	0.836	0.093	0.365	0.93
TS20	0.691	0.093	0.365	0.92
TS30	0.569	0.093	0.365	0.74

Note: R^2 = Coefficient of determination for *CSL* in the *e*-*p'* plane

(and consequently p') were calculated. Although the mixtures have similar void ratios and mean effective stresses, a different state parameter can be determined because of different position of the *CSLs*.

Several $CRR_{N=15}$ - Ψ curves were firstly identified for clean Ticino sand (Fig. 8) for each initial shear stress level. It is noted that almost all values of state parameters are lower than zero and thus a non flow-failure behaviour was observed during cyclic shearing test. The correlation between $CRR_{N=15}$ and $\Psi_{(0)}$ can be characterised fairly well by an exponential trend curve for a given α level, regardless of void ratio and effective confining stress, as follows:

$$CRR_{N=15} = a \bullet exp\left(-b \bullet \Psi\right) \tag{11}$$

where a and b are fitting parameters dependending on initial static shear stress ratio.

For each α value, the cyclic resistance ratio decreases with increasing state parameter. With increasing α, a clockwise rotation of the *CRR*-Ψ curves around a fixed pivot is observed. This means that the rate of strength reduction attributable to increasing contractiveness is always enhanced under greater α levels. In particular, it is identified a threshold Ψ value below which the cyclic resistance increases with increasing α (beneficial effect), whereas beyond which the cyclic resistance decreases with further increase of α (detrimental effect).

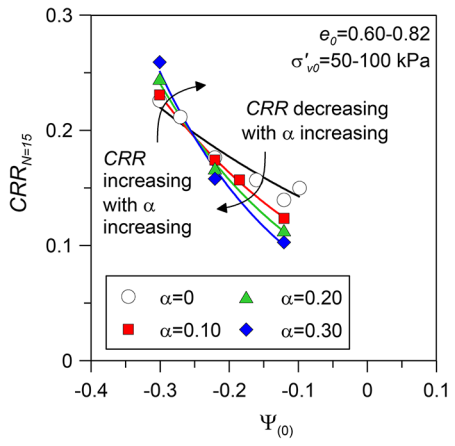

Fig. 8 *CRR*-Ψ correlations of clean Ticino sand under different α levels

Since the focus of the present study is to investigate sand-silt mixtures with fines content less than f_{thre}, which resulted equal to 24.5% (Fig. 4), in the following analysis only the data of *TS*, *TS10* and *TS20* were considered. Thus, for all *TS*-fines mixtures (f_c=0–20%) tested at different void ratios (e_0 = 0.51–0.82), initial vertical effective stresses (σ'_{v0}=50–100 kPa) and initial static shear stresses (α = 0-0.30), the cyclic resistance ratio $CRR_{N=15}$ has been plotted as a function of $\Psi_{(0)}$ in Fig. 9, together with the trend lines fitting the clean sand data previously depicted in Fig. 8. The results demonstrate that data points of silty sands under different α levels are located very close to the corresponding trend lines for clean Ticino sand, proving that the α-induced clockwise rotation of the *CRR*-Ψ curves shall apply to silty sands in cyclic simple shear tests. Using both clean and silty sand data, improved relationships (R^2 = 0.78–0.92) are depicted in Fig. 9 ("Trendlines for all f_c").

CRR - *Ψ** correlations under an initial static shear stress

For different fines contents of tested mixtures presented in Fig. 5, there are apparently separate *CRR*-*e* correlations. An important merit of the equivalent granular void ratio is to achieve a single and unified *CRR*-*e** correlation.

To optimise the b parameter of Eq. (9) (termed b_{best}), a b value was determined for a given initial static shear stress ratio by back-analysis of the *CRR*-*e** data, taking as reference the cyclic resistance curve of the clean sand. It was assumed b to be constant for all mixtures, thus four unified and consistent *CRR*-*e** correlations (i.e. *EG-CRRLs*) were defined for the four levels of initial static shear stress ratio α. It is interesting to note that the separate *CRR*–*e* curves with varying f_c depicted in Fig. 5 tend to collapse into a single *CRR*-*e** correlation close to that of zero fines content (for which $e^* = e$), as shown in Fig. 10. Since for a given α value the *EG-CRRL* is the same for the clean sand and the mixture, such a relationship can be obtained from laboratory testing performed on clean sand only or sand with single f_c, which requires far fewer tests to characterise cyclic resistance of sand-silt mixtures. For the set of the data in Fig. 10, the relationship between the b_{best} parameter (determined by the procedure described above) and the corresponding initial static shear stress ratio α is illustrated in Fig. 11(a). Since the values of b with varying α fall in a narrow range between 0.28 and 0.37, a single reasonable value of b = 0.324 could be practically assumed for all α levels, causing a good coincidence between *EG-CRRL* and *CRRL* of clean sand in the *CRR*-*e** plane (R^2 = 0.80–0.95).

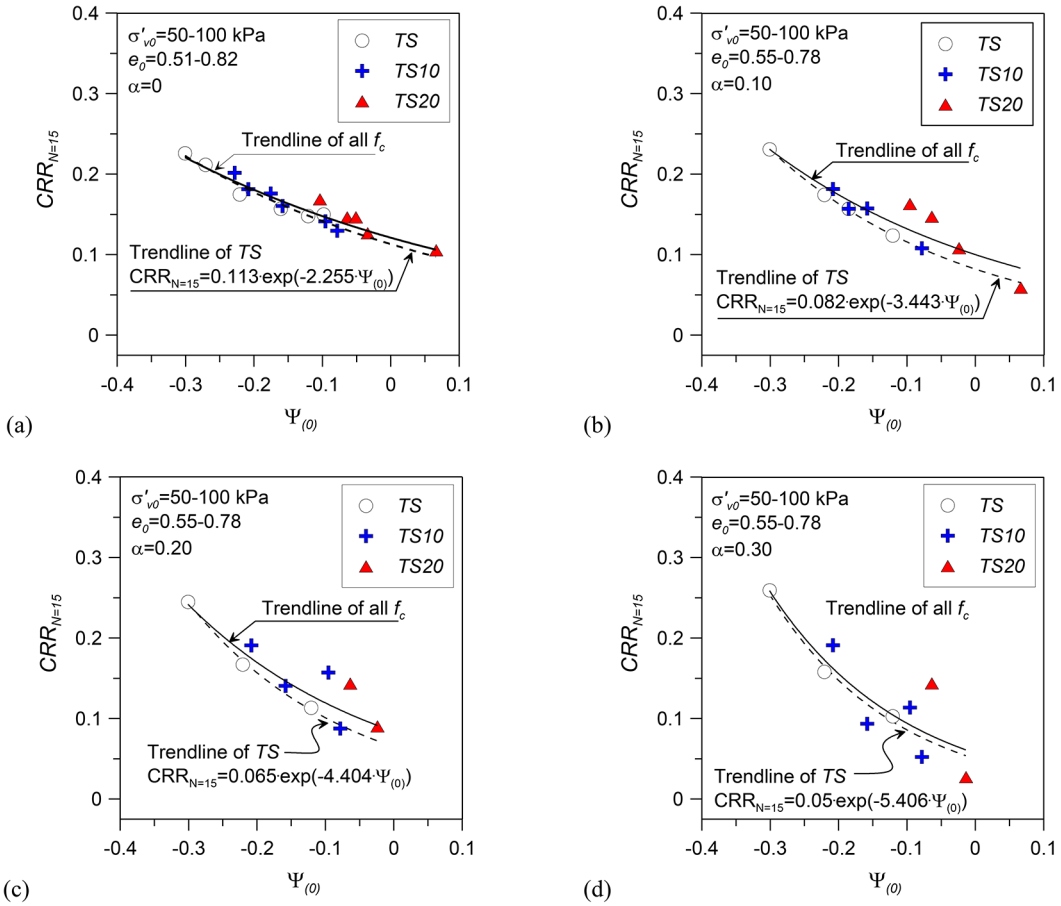

Fig. 9 *CRR-Ψ* correlations of Ticino sand-fines mixtures under different α levels

Figure 11(b) suggests that the value of b_{best} can be well predicted for any sand–fines mixture as a linear function of χ, at least for $\chi < 17$ and sands with grain shapes varying from rounded to sub-angular. Data points reported in this figure refer to the b_{best} values available or processed from the results of isotropically consolidated undrained cyclic triaxial tests (Rees 2010; Stamatopoulos 2010; Wei and Yang 2019a). In particular, for the cases of Stamatopoulos (2010) and Wei and Yang (2019a), due to the lack of back-analysed b value in the original publications, $CRR–e_0$ data were processed by the authors in the present study. Thus, such relationship will be a useful and reliable tool to predict b values from empirical correlations of sand-fines mixtures without performing a large number of undrained cyclic tests. Such a relationship could be even more improved if more and more data of b_{best} values are collected for different grading features and shapes of sand-fines mixtures.

To capture the combined effect of void ratio and initial effective confining stress, the equivalent granular state parameter, Ψ^*, defined in terms of e^* in place of e, was introduced. Ψ^* is evaluated in the e^*-logp' plane (Fig. 12) using Eq. (10).

A unique equivalent granular critical state line (*EG-CLS*) was obtained replacing e by e^* in critical state data for sand with $f_c < f_{thre}$ (Fig. 12). It was defined through the following equation:

$$e^*_{CS} = 0.958 - 0.071 \bullet (p'/P_a)^{0.452} \tag{12}$$

In this case the b_{mon} value was determined by back-analysis of the equivalent granular critical state (*EG-CSL*) data in the e^*-logp' plane, assuming the *CSL* of the clean sand as a reference soil response curve. An optimum b_{mon}= 0.237 for all Ticino sand-silt mixtures was calculated following this procedure. It would be noted that b may be loading mode-dependent, resulting in the present study b_{cyc} (Fig. 11a) higher than b_{mon}, consistently with previous studies (Rees 2010).

Figure 13 shows that for each α value there is a clear correlation between $CRR_{N=15}$ and Ψ^* which is practically unique, irrespective of fines content, void ratio and effective vertical stress. The relationship between cyclic resistance ratio and equivalent granular state parameter is given by the following equation:

$$CRR_{N=15} = c \bullet exp\left(-d \bullet \Psi^*\right) \tag{13}$$

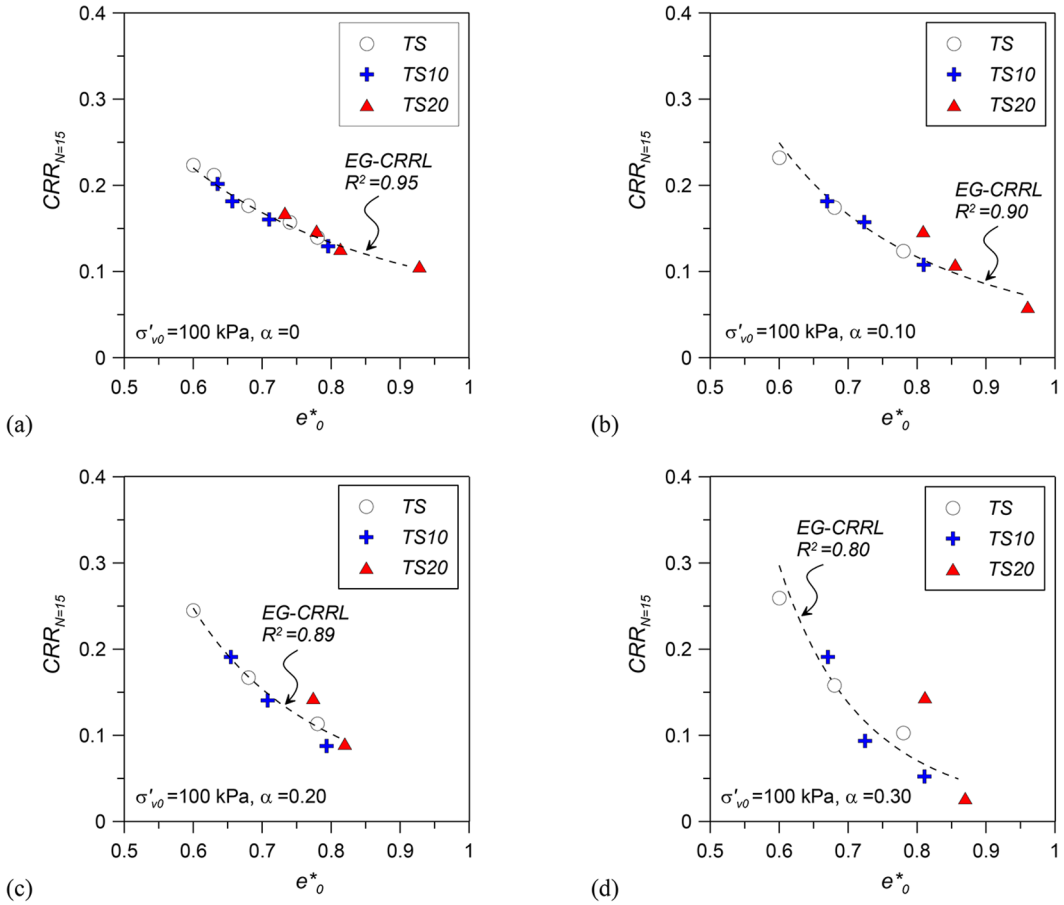

Fig. 10 Relationships between cyclic resistance ratio and e^* for TS-fines mixtures under different α values: (a) α=0, (b) α=0.10, (c) α=0.20 and (d) α=0.30

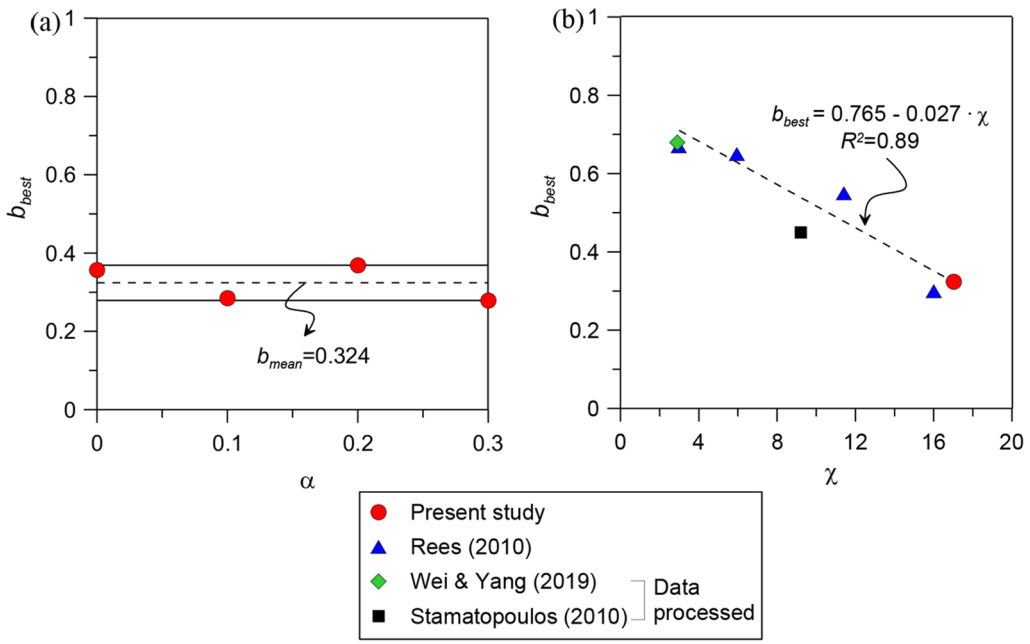

Fig. 11 Correlation of b_{best} with (a) initial static shear stress ratio α, (b) grading features of sand mixtures

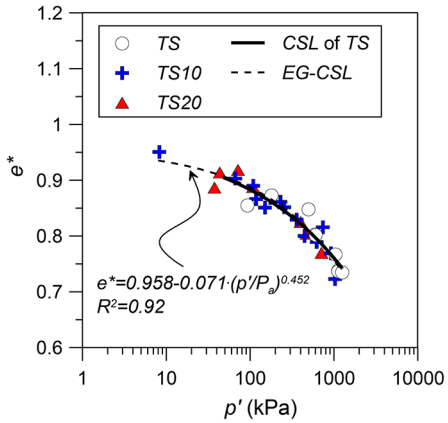

Fig. 12 Equivalent granular critical state line (*EG-CSL*) of *TS*-fines mixtures

where the coefficients c and d depend on static shear stress ratio, as follows:

$$c = 0.1116 - 0.2306 \bullet \alpha \; (R^2 = 0.98) \tag{14}$$

$$d = 2.001 + 13.773 \bullet \alpha \; (R^2 = 0.92)$$

Although some scatter data are observed for higher α values, namely $\alpha = 0.20$ and 0.30 in the figure, the exponential curves match the experimental data in a satisfactory manner. Thus, it is possible to predict the undrained cyclic resistance with the presence of an initial static shear stress based on state parameter and equivalent granular state parameter as well for assessing liquefaction potential of silty sands.

Provided that the b value is known, the equivalent state theory and the corresponding equivalent granular state parameter for non-plastic silty sands has the apparent benefit that it only requires the *EG-CSL*, which can be obtained on the basis of a limited number of test data performed on clean sands or a given mixture. It is worth mentioning that the relation between Ψ and Ψ^* can be expressed by the following equation:

$$\frac{\Psi}{\Psi^*} = 1 - (1 - b) \bullet f_c / 100 \tag{15}$$

which readily converts Ψ to Ψ^* or vice versa.

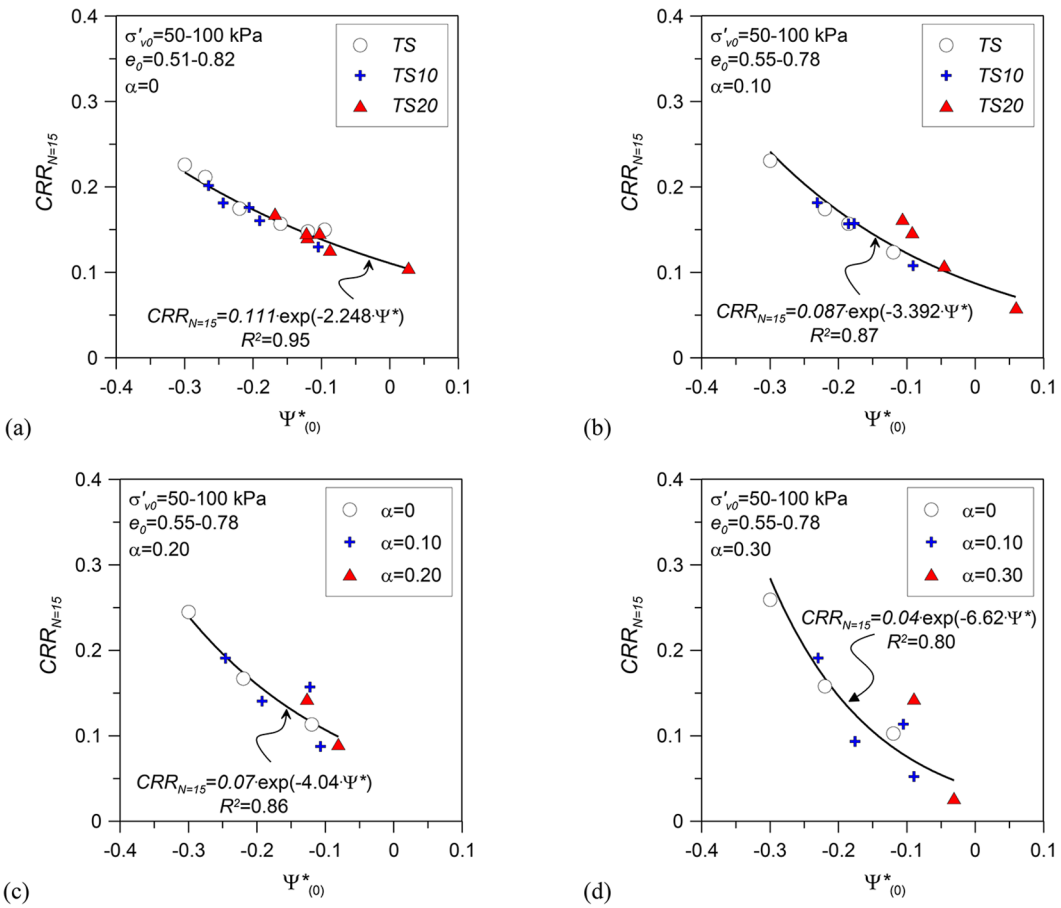

Fig. 13 CRR-Ψ^* correlations of Ticino sand with fines under different α levels

Predicting the failure modes of silty sands subjected to initial static shear stress based on Ψ^*

The deformation behaviour of silty sands under undrained cyclic loading in presence of an initial static shear stress can occur in three different forms: cyclic mobility, plastic strain accumulation and cyclic instability, the latter being also termed flow liquefaction/failure. The type of behaviour will depend on Ψ^* (or Ψ) as well as the applied cyclic stress (*CSR*) with respect to initial static shear stress ratio (α). Figure 14 illustrates the cyclic behaviour with the presence of an initial static shear stress of specimens having practically the same values of Ψ^* (<0) and α but different fines contents and void ratios. In particular, the shear stress vs. shear strain relationship [Fig. 14(a) and 14(c)] and effective stress path (*ESP*) [Fig. 14(b) and 14(d)] are depicted. Figure 14(a) and 14(b) show a typical failure pattern known as "cyclic mobility" (*CM*) which is characterised by a decrease in effective vertical stress due to the gradual increase of excess pore water pressure with loading cycles and finally the *ESP* reaches a quasi transient liquefied state (σ'_v=0) [Fig. 14(b)]. The shear strains develop in a cyclic pattern during loading but the soil does not collapse regaining its strength and stiffness due to dilation tendency up to a 3.75% single amplitude shear strain is reached for both specimens after a similar number of cycles [Fig. 14(a)].

On the other hand, Fig. 14(c) and 14(d) illustrate the plastic strain accumulation (*PSA*) type of behaviour of two specimens of *TS*-fines mixtures. The response exhibited by the two specimens is, again, very similar and it is characterised by plastic shear strains accumulated on the side of the applied initial static shear stress. The excess pore water pressure increases cyclically, but never equal to the initial effective vertical stress since the *ESP* remains far enough to the origin [Fig. 14(d)]. The above experimental observation illustrates that Ψ^*-based method represents a superior parameter to capture the overall undrained cyclic simple shear behaviour of tested soils with presence of an initial static shear stress.

Data points corresponding to the initial states relative to *EG-CSL* of all performed undrained cyclic SS tests are superimposed in e^*-logp' plane in Fig. 15(a). Overall, three bands of data points corresponding to flow, cyclic mobility and plastic strain accumulation located above or below the *EG-CSL* can be identified. In particular, it is evident from Fig. 15(a) that the data points clearly locate below the *EG-CSL* ($\Psi^*_{(0)}<0$), thus corresponding to non-flow behaviour as indicated by the symbol "cyclic mobility and plastic strain accumulation" (data of *TS* and *TS* with fines). On the other hand, the few data points (i.e. *TS20*) that correspond to flow or limited flow type behaviour ($\Psi^*_{(0)}>0$) are located above the *EG-CSL*. If such flow-type failure occurs in situ, it may cause catastrophic consequences because of its sudden nature. Thus, it is evident that the knowledge of *EG-CSL* can represent an effective tool to differentiate flow to non-flow pattern of behaviour of sand-silt mixtures ($f_c \leq f_{thre}$) when the initial state of sample is defined through $\Psi^*_{(0)}$. In the present study the values of $\Psi^*_{(0)}>0$ are in the range of 0.026 to 0.059 while the data points corresponding to $\Psi^*_{(0)}<0$ are in the range -0.301 to -0.046.

The next step is to examine which are the stress conditions (*CSR*, α) leading to a dominant type of undrained behaviour between *CM* and *PSA*. This is illustrated in Fig. 15(b) where it is evident that the deformation mechanism of the mixture depends on the magnitude of the initial static stress ratio (α) with respect to the applied cyclic stress ratio (*CSR*). It is clear that under no stress-reversal conditions (i.e. $\alpha/CSR \geq 1$), *PSA* always occurs. Apparently, an intermediate stress zone ($0.71<\alpha/CSR<1$, i.e. limited stress-reversal) dominated by *PSA* behaviour as well, was found to exist. The existence of a limited/intermediate stress condition was also identified in previous research from undrained cyclic triaxial tests (Pan and Yang 2018; Yang and Pan 2017) and simple shear tests (Tomasello and Porcino 2022) performed on clean sands. Finally, when α/CSR is <0.71 (case of shear stress-reversal condition), the *CM* behaviour is observed in all tests. The zero α/CSR ratio corresponds to the symmetrical loading case without any initial static shear stress. Thus, based on the magnitude of the static stress with respect to the applied cyclic stress, three typical patterns of loading namely stress reversal, no reversal and intermediate one, can be identified and a different deformational behaviour is expected to occur under undrained cyclic loading. The proposed method needs to be validated by using other types of sand-fines mixtures and a wider range of cyclic behaviours of materials to reach more definitive conclusions.

Estimating in-situ state parameter of silty sand from *CPT*

The most reliable direct method for determining the state parameters Ψ or Ψ^* is based on laboratory tests conducted on natural soils. As described in the present paper, a single unified correlation between *CRR* and Ψ or Ψ^* can be obtained for sand with different amounts of fines; an important advantage of Ψ^* against Ψ for the assessment of liquefaction potential of non-plastic silty sands in presence of an initial static shear stress is that the number of tests needed to establish the unified e^*-based *CSL* is much less than that required to assess a set of separate *CSLs* for sites where various f_c are involved.

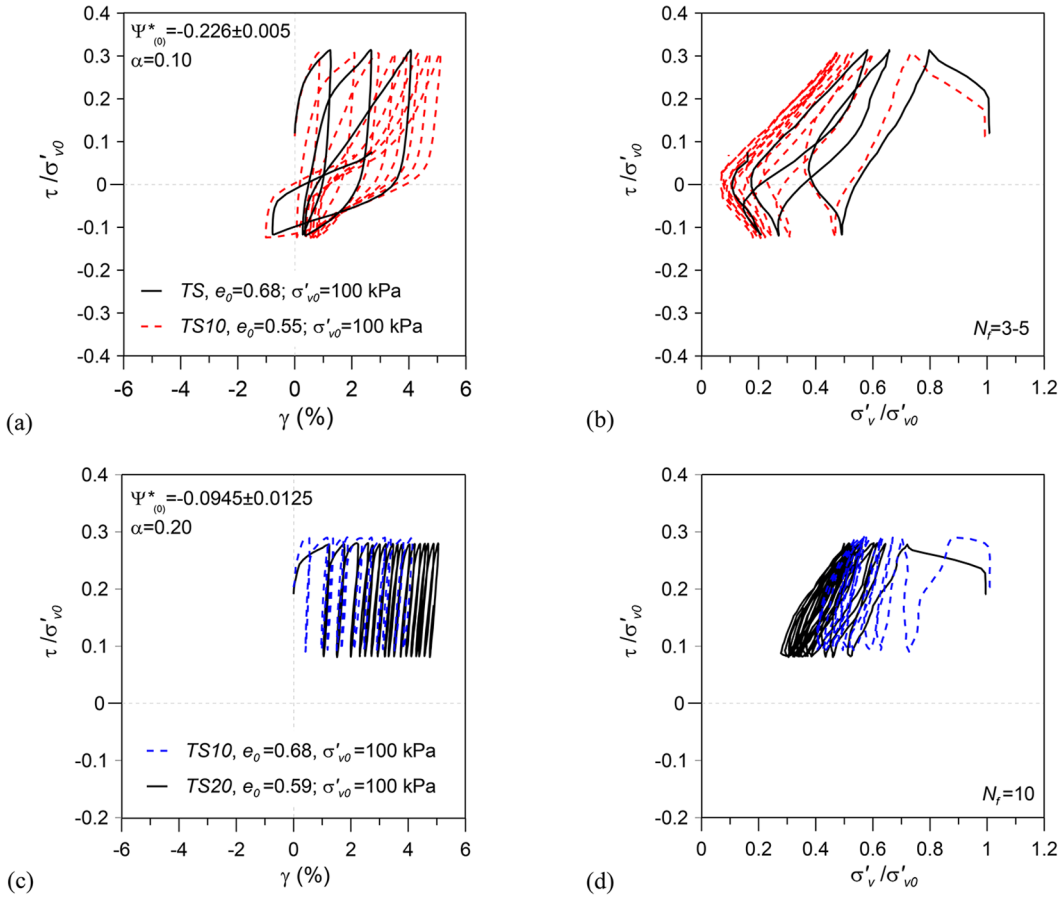

Fig. 14 Shear stress-shear strain relationship and effective stress path from cyclic simple shear tests on *TS*-fines mixtures with similar initial conditions ($\Psi^*_{(0)}$<0): (a) and (b) cyclic mobility, (c) and (d) plastic strain accumulation

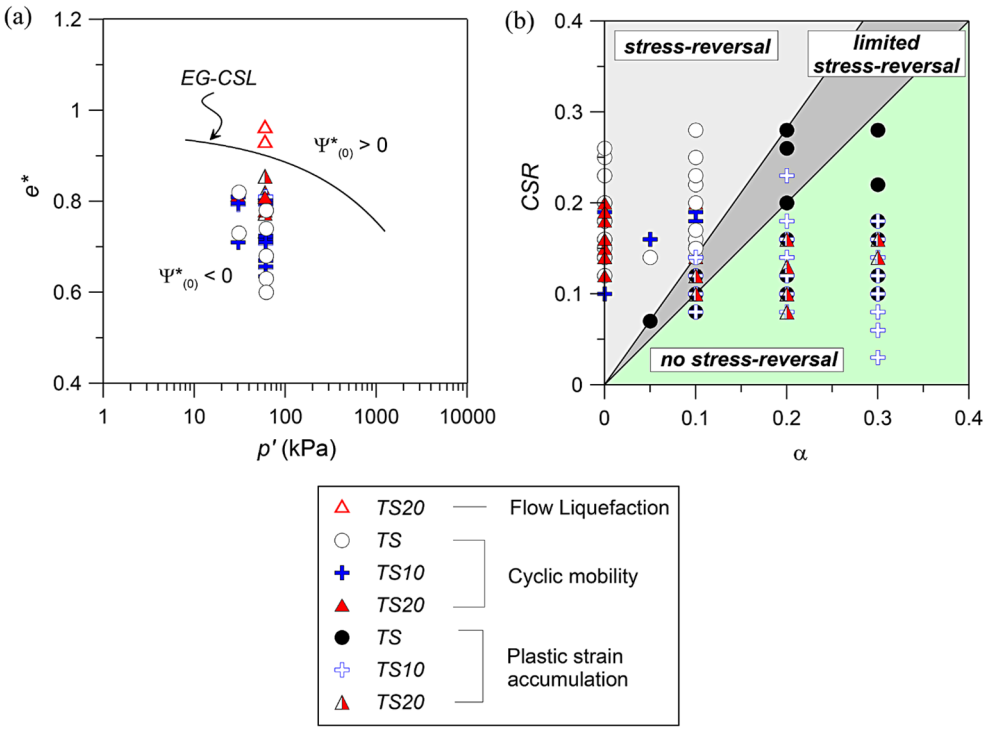

Fig. 15 (a) Initial positions of all the specimens tested in undrained cyclic simple shear tests and (b) zones of observed failure patterns

An alternative indirect method to estimate Ψ (or Ψ*) is to correlate them with in-situ tests such as field cone penetration tests (*CPTs*). Since cone penetration resistance of uncemented unaged soils is a function of material properties and state of soil (relative density and stress level), relationships were provided for sandy soils by several authors in order to evaluate the initial state parameter Ψ from the normalised cone resistance. Such studies were based on large calibration chamber (*CC*) (Been et al. 1986; Jefferies and Been 2016; Russell et al. 2022; Ayala et al. 2022) and centrifuge calibration *CPTs* (Fioravante and Giretti 2016; Fioravante et al. 2022) or alternatively through numerical studies (Jaeger et al. 2014). Such correlations, however, are still lacking (Huang 2016) and further efforts are still needed to obtain reliable correlations between normalised cone penetration resistance and state parameter for non-plastic/low plasticity silty sands.

Different equations for stress normalisation of *CPT* penetration resistance were proposed in the literature (Olsen and Malone 1988; Robertson 1999, 2010; Jamiolkowski et al. 2003; Idriss and Boulanger 2006). The normalised cone resistance Q_p (on a log scale) is plotted, for example, against Ψ in Fig. 16 (see Table 4) where a collection of trend lines from literature data are depicted for clean sands and silty sands. The penetration resistance normalised to mean effective stress, $Q_p=(q_c-p_0)/p'_0 \cong q_c/p'_0$ was correlated to Ψ through the equation (Been et al. 1986):

$$Q_p = k \bullet exp(-m \bullet \Psi) \tag{16}$$

where:

- m and k = dimensionless fitting parameters. The parameter m provides the contribution to dilatancy on the cone penetration resistance for a given Ψ value while k represents the Q_p value when $\Psi=0$;
- p_0 and p'_0 = mean total and effective stresses at a given depth, respectively.

Once the state parameter has been determined, the simple relation which readily converts Ψ to Ψ* (for $f_c < f_{thre}$) is given by Eq. (15). Note that the derivation of Ψ* through Eq. (15) requires only the knowledge of the fines content and grading features of sand-fines mixtures (χ parameter). For clean sands it is obvious that $\Psi = \Psi$*.

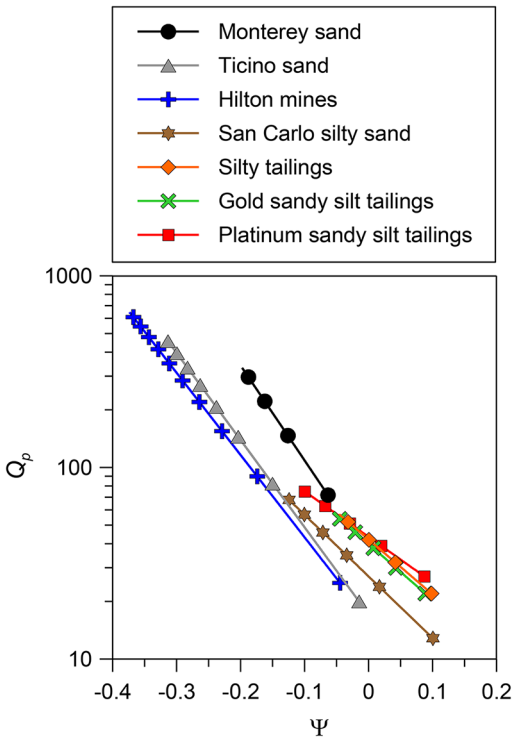

Fig. 16 Normalised cone penetration resistance Q_p versus state parameter Ψ for different sandy soils

It is apparent from Fig. 16 and Table 4 that m and k of Eq. (16) are material-dependent parameters; in particular, it was suggested (Been et al. 1987) that the constants k and m for sands were simple functions of the slope of *CSL* in the e-log(p') plane (i.e. λ parameter) while the presence of fines content reduces dilatancy effects and thus the value of m (Fioravante and Giretti 2016). Accordingly, the application of the described methodology would require further research to reach more definitive and well-established correlations between in-situ test results and the state parameter.

Table 4 Properties and fitting parameters of sandy soils reported in Fig. 16

Material	D_{50} (mm)	f_c (%)	k	m	Reference
Monterey sand (low compressibility)	0.37	0.12	34.8	11.4	Jefferies and Been (2016)
Ticino sand (moderate compressibility)	0.53	0.12	17.1	10.5	Jefferies and Been (2016)
Hilton mines (high compressibility)	0.20	2.5	16.1	9.9	Jefferies and Been (2016)
San Carlo silty sand	0.21	12.5	27	7.4	Fioravante and Giretti (2016)
Silty tailings	0.05–0.06	54–59	42.1	6.6	Russel et al. (2022)
Gold sandy silt tailings	0.05	58	39.9	6.7	Ayala et al. (2022)
Platinum sandy silt tailings	0.05	72	43.5	5.5	Ayala et al. (2022)

Conclusions

In the present study a comprehensive experimental program of undrained cyclic simple shear (*CSS*) tests was conducted on reconstituted samples of Ticino sand with fines (f_c=0–30%) at various initial states (e_0, σ'_{v0}) conditions, static shear stress ratio (α = 0-0.30) and cyclic stress levels. In particular, based on the magnitude of the initial static shear stress relative to the applied cyclic stress, three typical patterns of loading, namely stress reversal, no reversal and intermediate, were reproduced. A conceptual framework based on critical state and equivalent state theory was applied to predict cyclic failure patterns and cyclic resistance of non-plastic silty sands in a unified way. The following main conclusions are drawn from this study:

1. When adding silty fines to clean sand while maintaining e_0 and σ'_{v0} constant, the decrease of $CRR_{N=15}$ with f_c up to a threshold fines content (f_{thre}≅24.5%) is much more pronounced for tests with an initial static shear stress ($\alpha \neq 0$) compared to those with absence of α.
2. Initial (global) void ratio and effective vertical stress are the main factors influencing the failure patterns and cyclic resistance of sand-silt mixtures for a given α level. The cyclic resistance of sand-silt mixtures decreases with increasing void ratio and effective vertical stress, but the impact of these two variables on cyclic resistance can be altered by the presence of an initial static shear stress.
3. The undrained cyclic response and shear strength of silty sands ($f_c < f_{thre}$) can be evaluated through the state parameter Ψ and the equivalent granular state parameter Ψ*. Ψ* can be calculated provided the equivalent granular void ratio e* is introduced in place of e. A simple linear relationship is derived by processing and analysing additional published datasets of cyclic triaxial tests to determine b_{best} from the particle diameter ratio χ of sand-silt mixtures with sand grain shapes varying from rounded to sub-angular.
4. For a given static shear stress ratio, there is a good correlation between $CRR_{N=15}$ and Ψ (or Ψ*) for all mixtures ($f_c < f_{thre}$), void ratio and effective vertical stress (R^2 = 0.80–0.95) with the obvious advantage of unifying the cyclic shear strength response of silty sands. Such relationships are expressed by an exponential decreasing function which matches the experimental data in a satisfactory manner, especially when Ψ* is adopted. The *CRR*-Ψ (or Ψ*) curves are characterised by a clockwise rotation with increasing α.
5. The deformation behaviour of silty sands causing initial liquefaction in presence of an initial static shear stress can occur in three different patterns: cyclic mobility, plastic strain accumulation and cyclic instability, depending on the initial value of Ψ* and the applied α/CSR ratio. In the present study, plastic strain accumulation always occurs under no stress-reversal conditions (i.e. $\alpha/CSR \geq 1$), whereas the cyclic mobility behaviour is observed in all tests for shear stress-reversal condition (i.e. $\alpha/CSR < 0.71$). Additionally, an intermediate stress zone ($0.71 < \alpha/CSR < 1$, i.e. limited stress-reversal) is found to exist and it is dominated by *PSA* behaviour as well.

Finally, it is worth noting that the in-situ relationship between liquefaction resistance ratio and state parameter may, however, be different from that determined in laboratory due to some aspects, namely structure (fabric and bonding), stress history and ageing. Further efforts are still required to validate the proposed *CSSM*-based approach for non-plastic/low plasticity silty sands by field observations of liquefied sites and develop reliable correlations to obtain Ψ (or Ψ*) from in-situ test results [standard penetration test (*SPT*) and cone penetration test (*CPT*)].

The authors hope that this paper will trigger significant interest for further research on critical state approach to obtain definitive correlations between cyclic resistance and state parameter for non-plastic/low plasticity silty sands covering a wide range of sand-fines mixtures, specimen preparation methods and cyclic behaviours of materials (i.e. flow failure).

Nomenclature

a,b	fitting parameters of $CRR_{N=15} - \Psi_{(0)}$ correlation.
α	initial static shear stress ratio.
α_{th}	threshold initial static shear stress ratio.
b	fines influencing factor.
b_{best}	fines influencing factor obtained through trial and error procedure.
b_{cyc}	fines influencing factor obtained from cyclic tests.
b_{mean}	mean fines influencing factor.
b_{mon}	fines influencing factor obtained from monotonic tests.
c, d	fitting parameters of $CRR_{N=15} - \Psi^*_{(0)}$ correlation.
CC	calibration chamber.
CM	cyclic mobility.
CPT	cone penetration test.
CRR	undrained cyclic resistance.
$CRR_{N=15}$	cyclic stress ratio causing failure in 15 uniform loading cycles.
CRRL	cyclic resistance line.
CSL	critical state line.

CSR	cyclic stress ratio.
CSS	cyclic simple shear.
$CSSM$	critical state soil mechanics.
C_U	uniformity coefficient.
D_R	relative density.
DSS	direct simple shear.
D_{10}	diameter of sand grain at which 10% of sample is finer.
D_{50}	mean grain size.
d_{50}	mean particle diameter of fines.
$\Delta\sigma_v$	decrease (or increase) of vertical stress.
Δu	excess pore water pressure.
e	global void ratio.
e_0	initial global void ratio.
e^*	equivalent granular void ratio.
e_{CS}	critical void ratio.
e^*_{CS}	equivalent granular void ratio at critical state.
e^*_f	equivalent interfine void ratio.
e_Γ, λ_c, ξ	fitting parameters of the critical state line.
e_{max}	maximum void ratio.
e_{min}	minimum void ratio.
e_s	skeleton void ratio.
$EG\text{-}CRRL$	equivalent granular cyclic resistance line.
$EG\text{-}CSL$	equivalent granular critical state line.
ESP	effective stress path.
f_c	fines content.
f_{thre}	threshold fines content.
φ'	friction angle of soil.
φ'_{cs}	critical state friction angle of soil.
φ'_p	peak friction angle of soil.
G_S	specific gravity.
γ_{SA}	single amplitude shear strain.
γ_{peak}	peak shear strain.
K_0	coefficient of lateral earth pressure at rest.
K_α	correction factor for initial static shear stress.
K_σ	correction factor for overburden stress.
χ	particle diameter ratio.
$LVDT$	linear variable differential transducer.
λ	slope of CSL.
m, k	dimensionless fitting parameters of $Q_p - \Psi$ correlation.
M	critical state stress ratio.
M_c	critical state stress ratio under triaxial compression conditions.
M_w	earthquake magnitude.
NGI	Norwegian Geotechnical Institute.
p'	mean effective stress.
p_0	initial mean total stress.
p'_0	initial mean effective stress.
P_a	atmospheric pressure.
q	deviatoric stress.
q_c	cone resistance.
Q_p	normalised cone resistance.
PSA	plastic strain accumulation.
Ψ	state parameter.
$\Psi_{(0)}$	initial state parameter.
Ψ^*	equivalent granular state parameter.
$\Psi^*_{(0)}$	initial equivalent granular state parameter.
R^2	coefficient of determination.
SPT	standard penetration test.
SS	simple shear.
σ_h	total horizontal stress.
σ'_h	effective horizontal stress.
σ'_{h0}	initial effective horizontal stress.
σ_v	total vertical stress.
σ'_v	effective vertical stress.
σ'_{v0}	initial effective vertical stress.
τ_{cyc}	cyclic shear stress.
τ_{stat}	initial static shear stress.
TS	Ticino sand.
$TS10$	Ticino sand with 10% fines content.
$TS20$	Ticino sand with 20% fines content.
$TS30$	Ticino sand with 30% fines content.
w	moisture content.

Funding Open access funding provided by Università degli Studi Mediterranea di Reggio Calabria within the CRUI-CARE Agreement.

Declarations

Conflict of interest The authors declare no competing interests.

References

Alarcon-Guzman A, Leonards GA, Chameau JL (1988) Undrained monotonic and cyclic strength of sands. J Geotech Eng 114:1089–1109. https://doi.org/10.1061/(ASCE)0733-9410(1988)114:10(1089)

Ayala J, Fourie A, Reid D (2022) Improved cone penetration test predictions of the state parameter of loose mine tailings. Can Geotech J. https://doi.org/10.1139/cgj-2021-0460

Baki MAL, Rahman MM, Lo SR (2014) Predicting onset of cyclic instability of loose sand with fines using instability curves. Soil Dyn Earthq Eng 61–62:140–151. https://doi.org/10.1016/j.soildyn.2014.02.007

Been K, Jefferies MG (1985) A state parameter for sands. Géotechnique 35:99–112. https://doi.org/10.1680/geot.1985.35.2.99
Been K, Crooks JHA, Becker DE, Jefferies MG (1986) The cone penetration test in sand: part I, state parameter interpretation. Géotechnique 36:239–249. https://doi.org/10.1680/geot.1986.36.2.239
Been K, Jefferies MG, Crooks JHA, Rothenberg L (1987) The cone penetration test in sands: part II, General inference of state. Géotechnique 37:285–299. https://doi.org/10.1680/geot.1987.37.3.285
Been K, Jefferies MG, Hachey J (1991) The critical state of sands. Géotechnique 41:365–381. https://doi.org/10.1680/geot.1991.41.3.365
Bouckovalas GD, Andrianopoulos KI, Papadimitriou AG (2003) A critical state interpretation for the cyclic liquefaction resistance of silty sands. Soil Dynam Earthq Eng 23:115–125. https://doi.org/10.1016/S0267-7261(02)00156-2
Carraro JAH, Salgado R (2004) Mechanical Behavior of Non-Textbook Soils (Literary Review). Report Review No. FHWA/IN/JTRP-2004/5, Pardue University, West Lafayette, Indiana
Carraro JAH, Bandini P, Salgado R (2003) Liquefaction resistance of clean and nonplastic silty sands based on cone penetration resistance. J Geotech Geoenviron Eng 129:965–976. https://doi.org/10.1061/(ASCE)1090-0241-(2003)129:11(965)
Carrera A, Coop M, Lancellotta R (2011) Influence of grading on the mechanical behaviour of Stava tailings. Géotechnique 61:935–946. https://doi.org/10.1680/geot.9.P.009
Casagrande A (1936) Characteristics of cohesionless soils affecting the stability of earth fills. J Boston Soc Civil Eng 23:257–286
Castro G, Poulos SJ (1977) Factors affecting liquefaction and cyclic mobility. J Geotech Eng Div 103:501–516. https://doi.org/10.1061/AJGEB6.0000433
Chiaro G, Koseki J (2013) Prediction of earthquake-induced liquefaction for level and gently sloped ground. In: Chin CY (ed) 19th New Zealand geotechnical society symposium. Institution of Professional Engineers New Zealand, New Zealand, pp 61–68
Chien L-K, Oh Y-N, Chang C-H (2002) Effects of fines content on liquefaction strength and dynamic settlement of reclaimed soil. Can Geotech J 39:254–265. https://doi.org/10.1139/t01-083
Chu J, Leong WK (2002) Effect of fines on instability behaviour of loose sand. Géotechnique 52:751–755. https://doi.org/10.1680/geot.2002.52.10.751
da Viana A, Molina-Gómez F, Ferreira C (2022) Liquefaction resistance of TP-Lisbon sand: a critical state interpretation using in situ and laboratory testing. Bull Earthq Eng 21:767–790. https://doi.org/10.1007/s10518-022-01577-8
Dash HK, Sitharam TG (2009) Undrained cyclic pore pressure response of sand–silt mixtures: effect of nonplastic fines and other parameters. Geotech Geol Eng 27:501–517. https://doi.org/10.1007/s10706-009-9252-5
Dyvik R, Berre T, Lacasse S, Raadim B (1987) Comparison of truly undrained and constant volume direct simple shear tests. Géotechnique 37:3–10. https://doi.org/10.1680/geot.1987.37.1.3
Finn WDL (1985) Aspects of constant volume cyclic simple shear. In: Khosla V (ed) Advances in the art of testing soils under cyclic conditions. Herron Consultants, Cleaveland, pp 74–98
Finn WD, Vaid YP (1977) Liquefaction potential from drained constant volume cyclic simple shear tests. In: Prakashan S (ed), Proc 6th World Conference on Earthquake Engineering. Indian Society of Earthquake Technology, New Delhi, pp 7–12
Fioravante V, Giretti D (2016) State parameter of sands from centrifuge cone penetration test. In: Theorel L, Blanc M, Bretschneider A, Escoffier S (Eds) 3rd European Conference on Physical Modelling in Geotechnics. Institut Francais des Sciences et Technologies des Transports, de l'Amenagement et des Reseaux, Nantes, pp 1–6
Fioravante V et al (2022) Calibration cone penetration testing in silty soils. In: Gottardi G, Tonni L (Eds) Proceedings of the 5th International Symposium on Cone Penetration Testing (CPT'22). CRC Press, London, pp 420–426
Georgiannou VN, Burland JB, Hight DW (1990) The undrained behaviour of clayey sands in triaxial compression and extension. Géotechnique 40:431–449. https://doi.org/10.1680/geot.1990.40.3.431
Gobbi S, Reiffsteck P, Lenti L, d'Avila MPS, Semblat J-F (2022) Liquefaction triggering in silty sands: effects of non-plastic fines and mixture-packing conditions. Acta Geotech 17:391–410. https://doi.org/10.1007/s11440-021-01262-1
Goundarzy M, Rahman MM, König D, Schanz T (2016) Influence of non-plastic fines content on maximum shear modulus of granular materials. Soils Found 56:973–983. https://doi.org/10.1016/j.sandf.2016.11.003
Hsiao D-H, Phan VT-A (2016) Evaluation of static and dynamic properties of sand-fines mixtures through the state and equivalent state parameters. Soil Dynam Earthq Eng 84:134–144. https://doi.org/10.1016/j.soildyn.2016.02.006
Huang AB (2016) The Seventh James K. Mitchell lecture: characterization of silt/sand soils. In: Lehane BM, Acosta-Martínez HE, Kelly R (eds) Geotechnical and geophysical characterisation 5. Australian Geomechanics Society, Sydney, pp 3–18
Huang AB, Chuang SY (2011) Correlating cyclic strength with fines contents through state parameters. Soils Found 51:991–1001. https://doi.org/10.3208/sandf.51.991
Idriss IM, Boulanger RW (2006) Semi-empirical procedures for evaluating liquefaction potential during earthquakes. Soil Dynam Earthq Eng 26:115–130. https://doi.org/10.1016/j.soildyn.2004.11.023
Ishihara K (1993) Liquefaction on flow failure during earthquake. Géotechnique 43:351–415. https://doi.org/10.1680/geot.1993.43.3.351
Jaeger RA, DeJong JT, Boulanger RW, Maki IP (2014) Effects of state parameter, fines content, and overburden stress on CPT resistance in silty sands. In: Robertson PK, Cabal KI (Eds) Proceedings from the 3rd International Symposium on Cone Penetration Testing. The CPT'14 Organizing Committee, Las Vegas, pp 655–663
Jamiolkowski M, Lo Presti DCF, Manassero M (2003) Evaluation of Relative Density and Shear Strength from CPT and DMT. Soil Behavior and Soft Ground Construction. https://doi.org/10.1061/40659(2003)7
Jefferies M, Been K (2016) Soil liquefaction: a critical state approach. Taylor & Francis, New York
Keyhani R, Haeri SM (2013) Evaluation of the effect of anisotropic consolidation and principle stress rotation on undrained behavior of silty sands. Scientia Iranica 20:1637–1653
Kokusho T (2020) Earthquake-induced flow liquefaction in fines-containing sands under initial shear stress by lab tests and its implication in case histories. Soil Dynam Earthq Eng 130:105987. https://doi.org/10.1016/j.soildyn.2019.105984
Kuerbis R, Negussey D, Vaid YP (1988) Effect of gradation and fines content on the undrained response of sand. Geotech Special Publication 21:330–334
Ladd RS (1978) Preparing test specimens using undercompaction. Geotech Test J 1:16–23. https://doi.org/10.1520/GTJ10364J
Lashkari A (2014) Recommendations for extension and re-calibration of an existing sand constitutive model taking in to account varying non-plastic fines content. Soil Dynam Earthq Eng 61–62:212–238. https://doi.org/10.1016/j.soildyn.2014.02.012
Mohammadi A, Qadimi A (2015) A simple critical approach to predicting the cyclic and monotonic response of sands with different fines contents using the equivalent intergranular void ratio. Acta Geotechica 10:587–606. https://doi.org/10.1007/s11440-014-0318-z
Moussa AA (1975) Equivalent drained-undrained shearing resistance of sand to cyclic simple shear loading. Géotechnique 25:485–494. https://doi.org/10.1680/geot.1975.25.3.485

Ni Q, Tan TS, Dasari GR, Hight DW (2004) Contribution of fines to the compressive strength of mixed soils. Géotechnique 54:561–569. https://doi.org/10.1680/geot.2004.54.9.561

Olsen RS, Malone PG (1988) Soil classification and site characterization using the cone penetrometer test. In: de Ruiter J (Ed) Proceedings of the First International Symposium on Penetration Testing. A.A. Balkema, Brookfield, pp 887–893

Pan K, Yang ZX (2018) Effects of initial static shear on cyclic resistance and pore pressure generation of saturated sand. Acta Geotech 13:476–487. https://doi.org/10.1007/s11440-017-0614-5

Pan K, Zhou GY, Yang ZX, Cai YQ (2020) Comparison of cyclic liquefaction behavior of clean and silty sands considering static shear effect. Soil Dynam Earthq Eng 139:106338. https://doi.org/10.1016/j.soildyn.2020.106338

Pan XD, Chen JQ, Pan K, Xu X, Jiang JW, Yang ZX (2021) Cyclic flow behavior of anisotropically consolidated sand with a small amount of fines. Soil Dynam Earthq Eng 146:106778. https://doi.org/10.1016/j.soildyn.2021.106778

Park S-S, Nong Z-Z, Lee D-E (2020) Effect of vertical effective and initial static shear stresses on the liquefaction resistance of sands in cyclic direct simple shear tests. Soils Found 60:1588–1607. https://doi.org/10.1016/j.sandf.2020.09.007

Pitman TD, Robertson PK, Sego DC (1994) Influence of fines on the collapse of loose sands. Can Geotech J 31:728–739. https://doi.org/10.1139/t94-084

Polito CP (1999) The Effects of Non-Plastic and Plastic Fines on The Liquefaction of Sandy Soils. Dissertation, Virginia Polytechnic Institute and State University

Porcino D, Diano V (2016) Laboratory study on pore pressure generation and liquefaction of low-plasticity silty sandy soils during the 2012 earthquake in Italy. J Geotech Geoenviron Eng 142:04016048. https://doi.org/10.1061/(ASCE)GT.1943-5606.0001518

Porcino D, Caridi G, Malara M, Morabito E (2006) An automated control system for undrained monotonic and cyclic simple shear tests. In: DeGroot DJ, DeJong JT, Frost JD, Baise LG (eds) Geotechnical engineering in the information technology age. American Society of Civil Engineering, Reston, pp 185–190

Porcino DD, Tomasello G, Diano V (2018a) Key factors affecting prediction of seismic pore water pressures in silty sands based on damage parameters. Bull Earthq Eng 16:5801–5819. https://doi.org/10.1007/s10518-018-0411-z

Porcino DD, Diano V, Tomasello G (2018b) Effect of non-plastic fines on cyclic shear strength of sand under an initial static shear stress. In: Wu W, Yu H-S (ed), Proceeding of China-europe conference on geotechnical engineering, springer series in geomechanics and geoengineering. Cham Springer, Switzerland, pp 597–601

Porcino DD, Tomasello G, Wichtmann T (2019) An insight into the prediction of limiting fines content for mixtures of sand with non-plastic fines based on monotonic and cyclic tests. In: Moraci N, Silvestri F, 7th International Conference on Earthquake Geotechnical Engineering. CRC Press, Rome, pp 4540–4547

Porcino DD, Diano V, Triantafyllidis T, Wichtmann T (2020) Predicting undrained static response of sand with non-plastic fines in terms of equivalent granular state parameter. Acta Geotech 15:867–882. https://doi.org/10.1007/s11440-019-00770-5

Porcino DD, Triantafyllidis T, Whichtmann T, Tomasello G (2021) Application of a critical state approach to cyclic liquefaction resistance of sand-silt mixtures under cyclic simple shear loading. J Geotech Geoenviron Eng 147:04020177. https://doi.org/10.1061/(ASCE)GT.1943-5606.0002470

Porcino DD, Triantafyllidis T, Wichtmann T, Tomasello G (2022) Using different state parameters for characterizing undrained static and cyclic behavior of sand with non-plastic fines. Soil Dynam Earthq Eng 159:107318. https://doi.org/10.1016/j.soildyn.2022.107318

Rahman MM (2012) Modelling the behaviour of sand with fines using equivalent granular void ratio. In: Narsilio G, Arulrajah A, Kodikara J (eds), Proc of the 11th Australia New Zealand Conference on Geomechanics. Australian Geomechanics Society, Melbourne, pp 656–661

Rahman MM (2021) The state of art on equivalent state theory for silty sands. In: Sitharam TG, Jakka R, Kolathayar S (eds) Latest developments in geotechnical earthquake engineering and soil dynamics. Springer Transactions in Civil and Environmental Engineering, Singapore, pp 225–246

Rahman MM, Lo SR (2008) The prediction of equivalent granular steady state line of loose sand with fines. Geomech Geoeng 3:179–190. https://doi.org/10.1080/17486020802206867

Rahman MM, Lo SR (2014) Undrained behavior of sand-fines mixtures and their state parameter. J Geotech Geoenviron Eng 140:04014036. https://doi.org/10.1061/(ASCE)GT.1943-5606.0001115

Rahman MM, Sitharam TG (2020) Cyclic liquefaction screening of sand with non-plastic fines: critical state approach. Geosci Front 11:429–438. https://doi.org/10.1016/j.gsf.2018.09.009

Rees SD (2010) Effects of fines on the undrained behaviour of Christchurch sandy soils. Dissertation, University of Canterbury

Robertson PK (1999) Estimation of minimum undrained shear strength for flow liquefaction using the CPT. In: Seco PS, Pinto (Eds) Proceedings of the Second International Conference on Earthquake Geotechnical Engineering. Balkema, Rotterdam, pp 1021–1028

Robertson PK (2010) Evaluation of Flow Liquefaction and Liquefaction Strength using the cone penetration test. J Geotech Geoenviron Eng 136:842–853. https://doi.org/10.1061/(ASCE)GT.1943-5606.0000286

Roscoe KH, Schofield AN, Wroth CP (1958) On the Yielding of soils. Géotechnique 8:22–53. https://doi.org/10.1680/geot.1958.8.1.22

Russel AR, Ayala TV, Wang Y, Reid D, Fourie AB (2022) Cone penetration tests in saturated and unsaturated silty tailings. https://doi.org/10.1680/jgeot.21.00261. Géotechnique

Sivathayalan D, Ha D (2011) Effect of static shear stress on the cyclic resistance of sands in simple shear loading. Can Geotech J 48:1471–1484. https://doi.org/10.1139/t11-056

Stamatopoulos CA (2010) An experimental study of the liquefaction strength of silty sands in terms of the state parameter. Soil Dynam Earthq Eng 30:662–678. https://doi.org/10.1016/j.soildyn.2010.02.008

Thevanayagam S (1998) Effect of fines and confining stress on undrained shear strength of silty sands. J Geotech GeoEnviron Eng 124:479–491. https://doi.org/10.1061/(ASCE)1090-0241(1998)124:6(479)

Thevanayagam S (2000) Liquefaction potential and undrained fragility of silty soils. In: Park R (ed) Proc 12th World conf on Earthquake Engineering. Society of Earthquake Engineering, Wellington, New Zealand, pp 1–8

Thevanayagam S, Martin GR (2002) Liquefaction in silty soils-screening and remediation issues. Soil Dynam Earthq Eng 22:1035–1042. https://doi.org/10.1016/S0267-7261(02)00128-8

Thevanayagam S, Shentan T, Mohan S, Liang J (2002) Undrained Fragility of Clean sands, Silty Sands, and Sandy Silts. J Geotech Geoenviron Eng 128:849–859. https://doi.org/10.1061/(ASCE)1090-0241(2002)128:10(849)

Tomasello G, Porcino DD (2022) Influence of sloping ground conditions on cyclic behavior of sand under simple shear loading. Soil Dynam Earthq Eng 163:107516. https://doi.org/10.1016/j.soildyn.2022.107516

Tomasello G, Porcino DD (2023) Earthquake-induce large deformation and failure mechanisms of silty sands in sloped ground conditions. Soil Dynam Earthq Eng 173:108056. https://doi.org/10.1016/j.soildyn.2023.108056

Vaid YP, Stedman JD, Sivathayalan S (2001) Confining and static shear effects in cyclic liquefaction. Can Geotech J 38:580–591. https://doi.org/10.1139/t00-120

Wei X, Yang J (2019a) Characterizing the effects of fines on the liquefaction resistance of silty sands. Soils Found 59:1800–1812. https://doi.org/10.1016/j.sandf.2019.08.010

Wei X, Yang J (2019b) Cyclic behavior and liquefaction resistance of silty sands with presence of initial static shear stress. Soil Dynam Earthq Eng 122:274–289. https://doi.org/10.1016/j.soildyn.2018.11.029

Wei X, Guo Y, Yang J, Guo C (2018) Liquefaction characteristics of four Ya-An low-plastic silty sands with presence of initial static shear stress. In: Qiu T, Tiwari B, Zhang Z (eds) Proc GeoShanghai 2018 Int Conf Adv Soil Dyn Found Eng. Springer, Shanghai, pp 62–69

Wei X, Yang J, Zhou Y-G, Chen Y (2020) Influence of particle-size disparity on cyclic liquefaction resistance of silty sands. Géotech Lett 10:155–161. https://doi.org/10.1680/jgele.19.00076

Wei X, Yang Z, Yang J (2023) Cyclic failure characteristics of silty sands with the presence of initial static shear stress. Soil Dynam Earthq Eng 171:107909. https://doi.org/10.1016/j.soildyn.2023.107909

Xu L-Y, Cai F, Chen W-Y, Zhang J-Z, Pan D-D, Wu Q, Chen G-X (2021) Undrained cyclic response of a dense saturated sand with various grain sizes and contents of nonplastic fines: experimental analysis and constitutive modeling. Soil Dynam Earthq Eng 145:106727. https://doi.org/10.1016/j.soildyn.2021.106727

Yan C, Shen Y, Zhao W, Sun Y (2023) State index for interpreting the state-dependent Behaviour of Granular Soil: a review. Arch Comput Methods Eng 30:4379–4399. https://doi.org/10.1007/s11831-023-09941-w

Yang ZX, Pan K (2017) Flow deformation and cyclic resistance of saturated loose sand considering initial static shear effect. Soil Dynam Earthq Eng 92:68–78. https://doi.org/10.1016/j.soildyn.2016.09.002

Yang J, Sze HY (2011a) Cyclic behaviour and resistance of saturated sand under non-symmetrical loading conditions. Géotechnique 61:59–73. https://doi.org/10.1680/geot.9.P.019

Yang J, Sze HY (2011b) Cyclic strength of sand under sustained shear stress. J Geotech Geoenviron Eng 137:1275–1285. https://doi.org/10.1061/(ASCE)GT.1943-5606.0000541

Yang S, Lacasse S, Sandven R (2006) Determination of the transitional fines content of mixtures of sand and non-plastic fines. Geotech Test J 29:102–107. https://doi.org/10.1520/GTJ14010

Yang J, Wei LM, Dai BB (2015) State variables for silty sands: global void ratio or skeleton void ratio? Soils Found 55:99–111. https://doi.org/10.1016/j.sandf.2014.12.008

Youd TL et al (2001) Liquefaction resistance of soils: summary report from the 1996 NCEER and 1998 NCEER/NSF workshops on evaluation of liquefaction resistance of soils. J Geotech Geoenviron Eng 127:817–833. https://doi.org/10.1061/(ASCE)1090-0241(2001)127:10(817)

Zhou GY, Pan K, Yang ZX (2023) Energy-based assessment of cyclic liquefaction behavior of clean and silty sand under sustained initial stress conditions. Soil Dynam Earthq Eng 164:107609. https://doi.org/10.1016/j.soildyn.2022.107609

Zhu Z, Dupla J-C, Canou J, Foester E (2022) Experimental study of liquefaction resistance: effect of non-plastic silt content on sand matrix. Eur J Environ Civil Eng 26:2671–2689. https://doi.org/10.1080/19648189.2020.17651980

Zuo L, Baudet BA (2015) Determination of the transitional fines content of sand-non plastic fines mixtures. Soils Found 55:213–219. https://doi.org/10.1016/j.sandf.2014.12.017

Zuo K, Gu X, Zhang J, Wang R (2023) Exploring packing density, critical state, and liquefaction resistance of sand-fines mixtures using DEM. Comput Geotech 156:105278. https://doi.org/10.1016/j.compgeo.2023.105278